

For Reference

NOT TO BE TAKEN FROM THIS ROOM

For Reference

NOT TO BE TAKEN FROM THIS ROOM

Ex LIBRIS
UNIVERSITATIS
ALBERTAENSIS





Digitized by the Internet Archive
in 2018 with funding from
University of Alberta Libraries

<https://archive.org/details/Goble1963>

37
3 (F)
THE UNIVERSITY OF ALBERTA

A SEARCH FOR A PROPOSED NEW LEVEL
OF Be^7

A THESIS

SUBMITTED TO THE FACULTY OF GRADUATE STUDIES
IN PARTIAL FULFILMENT OF THE REQUIREMENTS FOR THE DEGREE
OF MASTER OF SCIENCE

DEPARTMENT OF PHYSICS

by

DAVID FRANKLIN GOBLE

EDMONTON, ALBERTA

SEPTEMBER, 1963

ABSTRACT

Chesterfield and Spicer have applied the rotational model to Li^7 and have obtained quantitative agreement with experiment. The validity of the application of this model rests upon the existence of a $3/2^-$ state predicted at an excitation energy of 5.62 MeV. A search has been made for the mirror analogue of this level in Be^7 . The yield of gamma rays from the reaction $\text{Li}^6(p,\gamma)\text{Be}^7$ was investigated but no evidence of a resonance could be found in the region $E_p = 200 \text{ keV} - 450 \text{ keV}$. Spectra taken at $E_p = 800 \text{ keV}$ and $E_p = 400 \text{ keV}$ are in agreement with the results of Warren et al for the gamma de-excitation of the broad 6.35 MeV level, but a spectrum taken at $E_p = 300 \text{ keV}$ would seem to indicate that some other process is being observed.

ACKNOWLEDGEMENTS

I would like to express my thanks to the many people who helped to make this thesis possible.

I would first like to thank the Professors of the Nuclear Research Group; Doctors G. C. Neilson, W. K. Dawson, J. T. Sample, and D. W. Braben. I would particularly like to thank my supervisor Dr. D. W. Braben for suggesting this project and for the many suggestions, and generous help at all stages.

I would like also to express my thanks to the technicians; Lars Holm, who helped with the electronics, and Con Green who built the bombarding chamber.

I wish to thank as well A. Reedyk who assisted with the running of the accelerator, and my wife who drew many of the graphs and typed the final manuscript.

Finally, I would like to thank the National Research Council of Canada for the award of a Bursary.

TABLE OF CONTENTS

INTRODUCTION	1
SECTION 1. EXPERIMENTAL APPARATUS	3
Targets	3
Detector	5
General Description of Apparatus	8
SECTION 2. PREVIOUS WORK AND RESULTS	10
Previous Work	10
Results	15
Discussion	21
SECTION 3. ROTATIONAL MODEL	23
Rotational Model	23
Application to Li^7	40
SECTION 4. THE EXISTENCE OF THE PROPOSED NEW LEVEL OF Be^7	50

INTRODUCTION

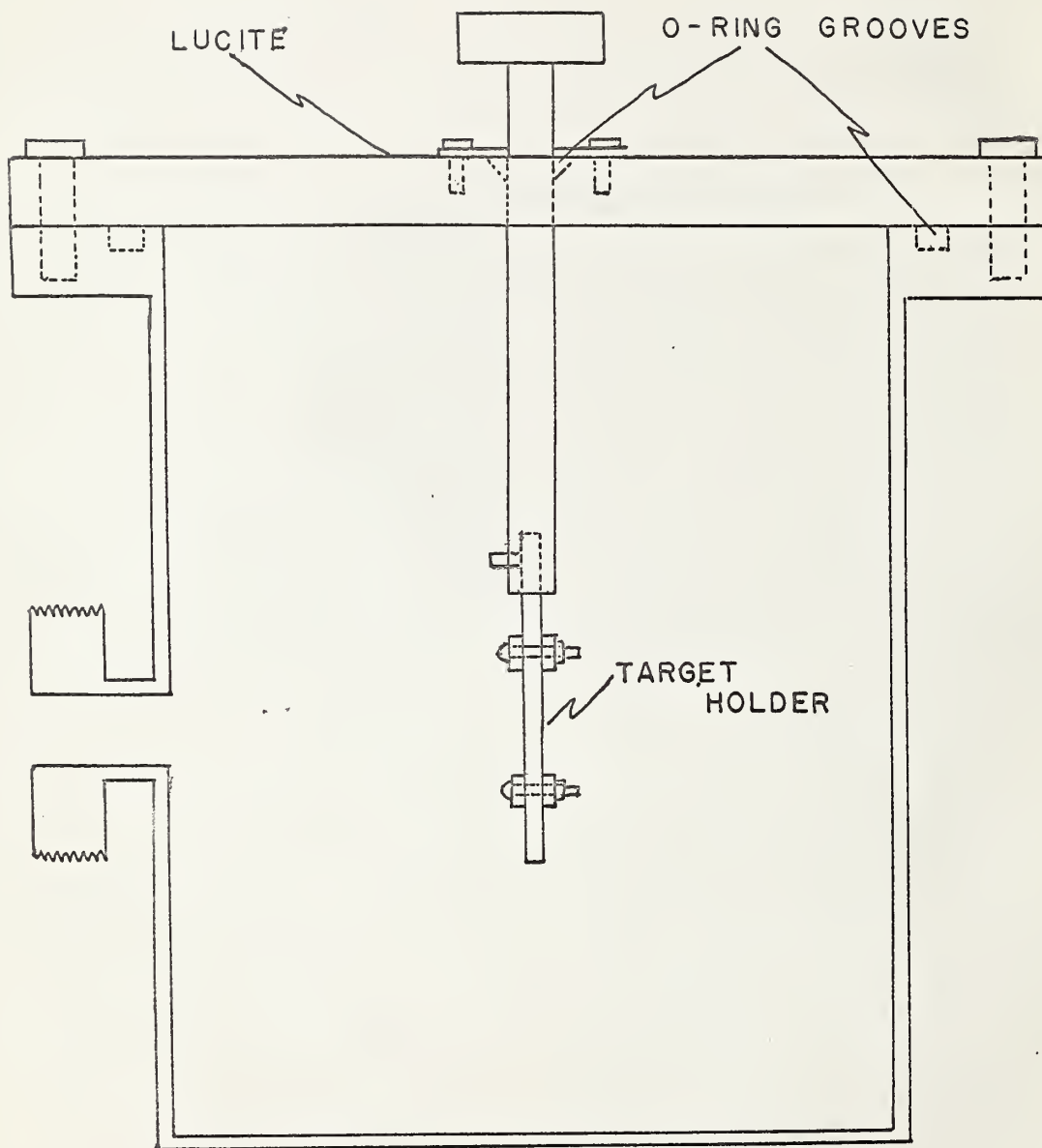
It has been known for some time that the rotational model provides an excellent fit to the experimental data on nuclei in the regions $155 \leq A \leq 185$, and $A \geq 225$; and it has recently been determined that nuclei with $A \approx 25$ also exhibit rotational spectra (Bo55, Li56, Br62). It has now been further suggested (Ke59) that the known low lying energy levels in the mirror nuclei Li^7 and Be^7 might form a rotational spectrum which is in agreement with the predictions of this model.

Following a procedure similar to that outlined by Nilsson (Ni55), Chesterfield and Spicer (Ch63) have fitted a theoretical rotational spectrum to the experimentally determined energy level spectrum of Li^7 . Quantitative agreement between the two spectra has been obtained. However, a necessary consequence of this fit has been the prediction of a $3/2^-$ level at an excitation energy of about 5.6 MeV in Li^7 . This state is not listed in the compilation of Ajzenberg-Selove and Lauritsen (Aj59), although there is a certain amount of experimental evidence which points to the existence of such a state. (For a discussion of this evidence see Section 2).

This thesis is a description of an experiment which

was performed in an attempt to resolve the problem presented by the conflicting evidence as to the existence of this state. Using the reaction $\text{Li}^6(\text{p}, \gamma)\text{Be}^7$ a search has been made for evidence of the Be^7 mirror analogue to the proposed 5.62 MeV ($3/2^-$) level of Li^7 .

In Section 1 the experimental apparatus and the general techniques used in the course of the experiment will be described; Section 2 is a discussion of some of the previous related work and the experimental results which were obtained; Section 3 consists of a description of the rotational model and a resume of its application to Li^7 as given by Chesterfield and Spicer (Ch63). Finally, Section 4 is a brief statement of the conclusions drawn from the experiment.



BOMBARDING CHAMBER

SECTION 1. EXPERIMENTAL APPARATUS

Targets

The targets used in this experiment consisted of isotopically separated Li^6 deposited to a thickness of about 200 $\mu\text{gms}/\text{cm}^2$ on a platinum backing. They were supplied by the Atomic Energy Research Establishment, Harwell, where they were prepared in vacuo and then shipped in glass vacuum bottles.

The first of the targets used was transferred from its vacuum container to the bombarding chamber in a dry box filled with argon to atmospheric pressure. The purity of the argon gas within the dry box was checked by means of a freshly cut block of ordinary lithium. The target was not removed from its vacuum bottle until this lithium block retained its freshly cut metallic luster after having been in contact with the argon gas for at least one hour. Once the target had been placed in the bombarding chamber, the chamber was immediately pumped down to a pressure of about 20 microns and then refilled with pure argon to a pressure of about two atmospheres. The target was kept isolated in this manner until it was ready to be used, when the bombarding chamber was placed on the beam tube of the accelerator and once again pumped down, this

time to a working pressure of approximately 7 microns. The bombarding chamber was maintained at this pressure for the rest of the time that the target was in use. To assist in keeping the target free from impurities a cold trap was mounted immediately in front of the bombarding chamber.

Reedyk (Re63) has examined the charged particle spectra resulting from the bombardment by deuterons of Li^6 deposited on thin nickel foils and has found that the only contaminants which are present in noticable amounts are C^{12} and O^{16} , even after these targets have been exposed to the atmosphere for relatively long periods of time. The 2,365 MeV level of N^{13} and the 0,500 MeV level of F^{17} are the only states that it would be possible to form when the nuclei C^{12} and O^{16} are bombarded by protons with energies below 2 MeV. On the basis of this it was decided to use one target which had simply been removed from its vacuum container and placed in the bombarding chamber without any attempt being made to keep it free from atmospheric impurities. This was done, and no difference was noted in the spectra taken with this target and those observed with the target which had been transferred in the argon environment. As far as could be determined the fluorine contamination remained at a constant level, and no impurities other than C^{12} and O^{16} could be found. For this reason all further targets which were used were transferred from their vacuum

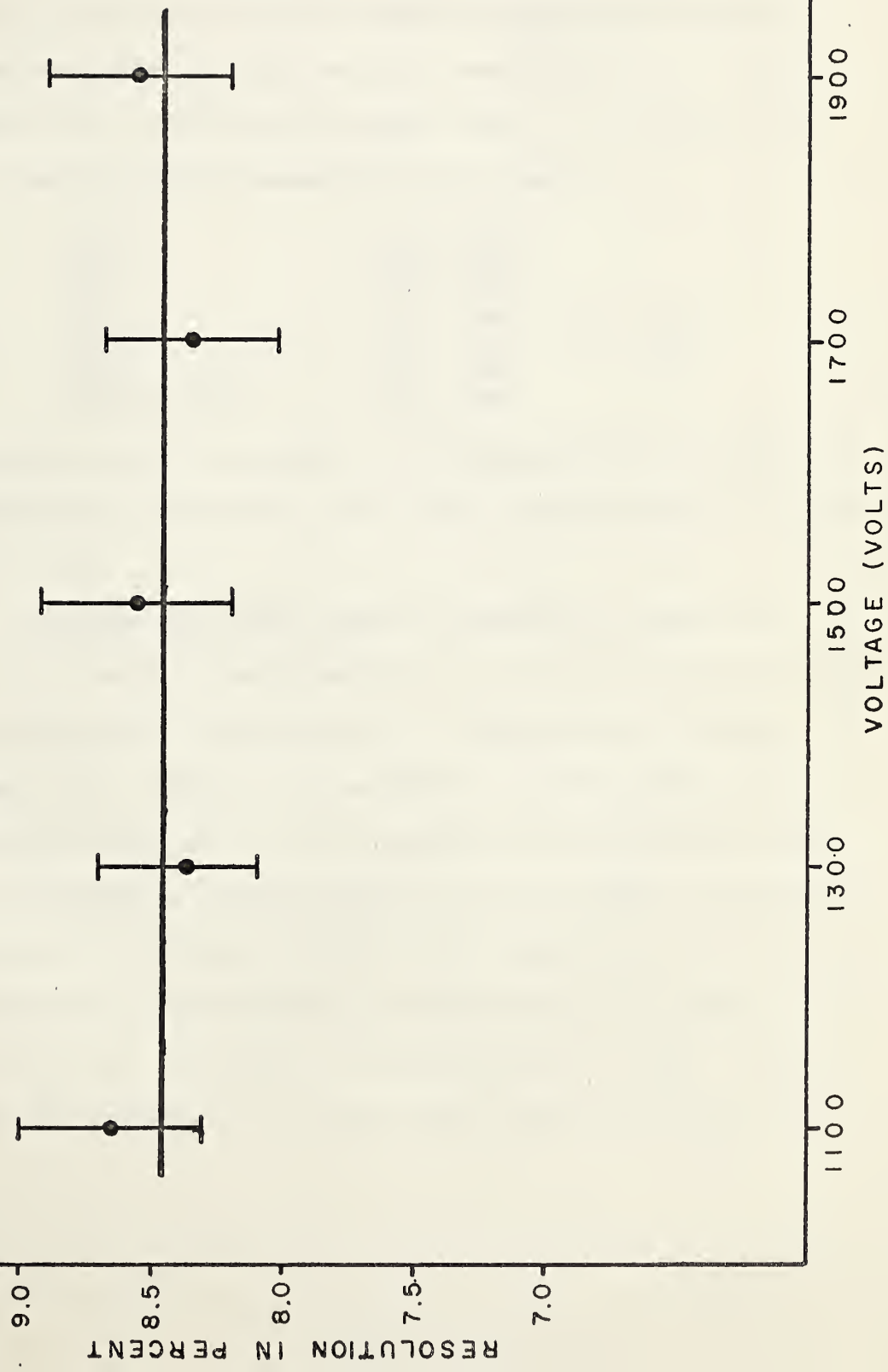
containers to the bombarding chamber in direct contact with the atmosphere.

In addition to the Li^6 target a F^{19} target (CaF_2 on a nickel backing) was also mounted in the bombarding chamber, on the back of the target holder. The bombarding chamber was so constructed as to make it possible to place either the fluorine or the lithium target in the beam by rotating the target holder. It was thus possible to calibrate the system by means of the reaction $\text{F}^{19}(\text{p}, \alpha \gamma) \text{O}^{16}$, rotate the target holder, and then examine the gamma rays resulting from the bombardment of the lithium target.

Detector

The gamma ray detector used in this experiment was supplied by Quartz-Silice, and consisted of a 3" x 3" $\text{NaI}(\text{Tl})$ scintillation crystal factory mounted directly onto a Phillips 54AVP photomultiplier tube. Measurements of the resolution of the detector were made with the voltage applied to the tube being varied from 1100 volts to 1900 volts with no significant change being noted (see Figure 1-1). During the course of the experiment the voltage was maintained at 1410 volts. With this voltage applied to the photomultiplier the resolution for the 0.662 MeV gamma ray of Cs^{137} was measured and found to be 8.38%. Also measured at this voltage was the ratio, for Co^{60} , of the height of the 1.33 MeV gamma ray peak to the minimum value attained in the trough between

Figure 1-1
Detector Resolution



this peak and that due to the 1.17 MeV gamma ray. This ratio was found to be 5.55:1. Both the resolution of the 0.662 MeV gamma ray of Cs^{137} and the peak-to-valley ratio for the 1.17 MeV and 1.33 MeV gamma rays of Co^{60} were checked periodically and were found to remain essentially constant.

The response of this detector was checked and found to be linear over the above voltage range. In checking the linearity the following gamma rays were used:

Co^{57}	0,136 MeV,
Cs^{137}	0,662 MeV,
Mn^{54}	0,835 MeV,
Na^{22}	0.51 MeV, 1,274 MeV,
Co^{60}	1,17 MeV, 1,33 MeV,
RdTh	2,62 MeV,
$\text{F}^{19}(\text{p},\alpha\gamma)\text{O}^{16}$	6,13 MeV,

Figures 1-2, 1-3, and 1-4 are respectively typical spectra obtained from Cs^{137} , Co^{60} , and the reaction $\text{F}^{19}(\text{p},\alpha\gamma)\text{O}^{16}$ at $E_p = 874$ keV.

To increase the real count to background ratio the scintillation crystal was sheathed in a 4" thick lead cylinder and the rest of the detector in a 2" thick lead cylinder. Even though this reduced the background considerably, a relatively large number of 1.46 MeV gamma rays were noted in the background spectrum. (These gamma rays presumably arose from the presence of radioactive K^{40} in the cement walls and floor).

Whenever a scintillation counter detects a gamma ray it does so indirectly by means of interactions in which charged particles are produced. In the energy range of interest in

Figure 1-2
 Cs^{137} Spectrum

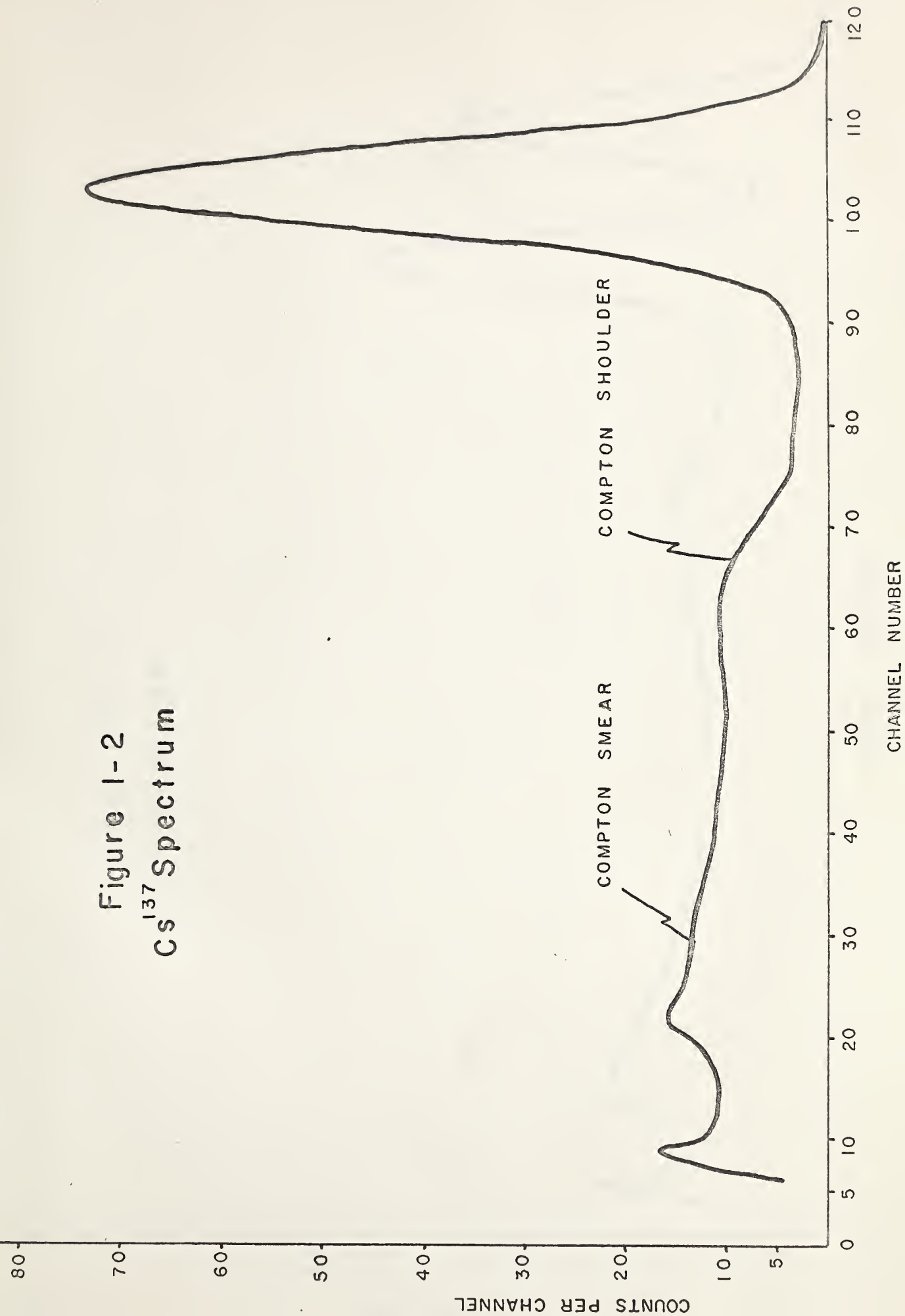


Figure 1-3
 Co^{60} Spectrum

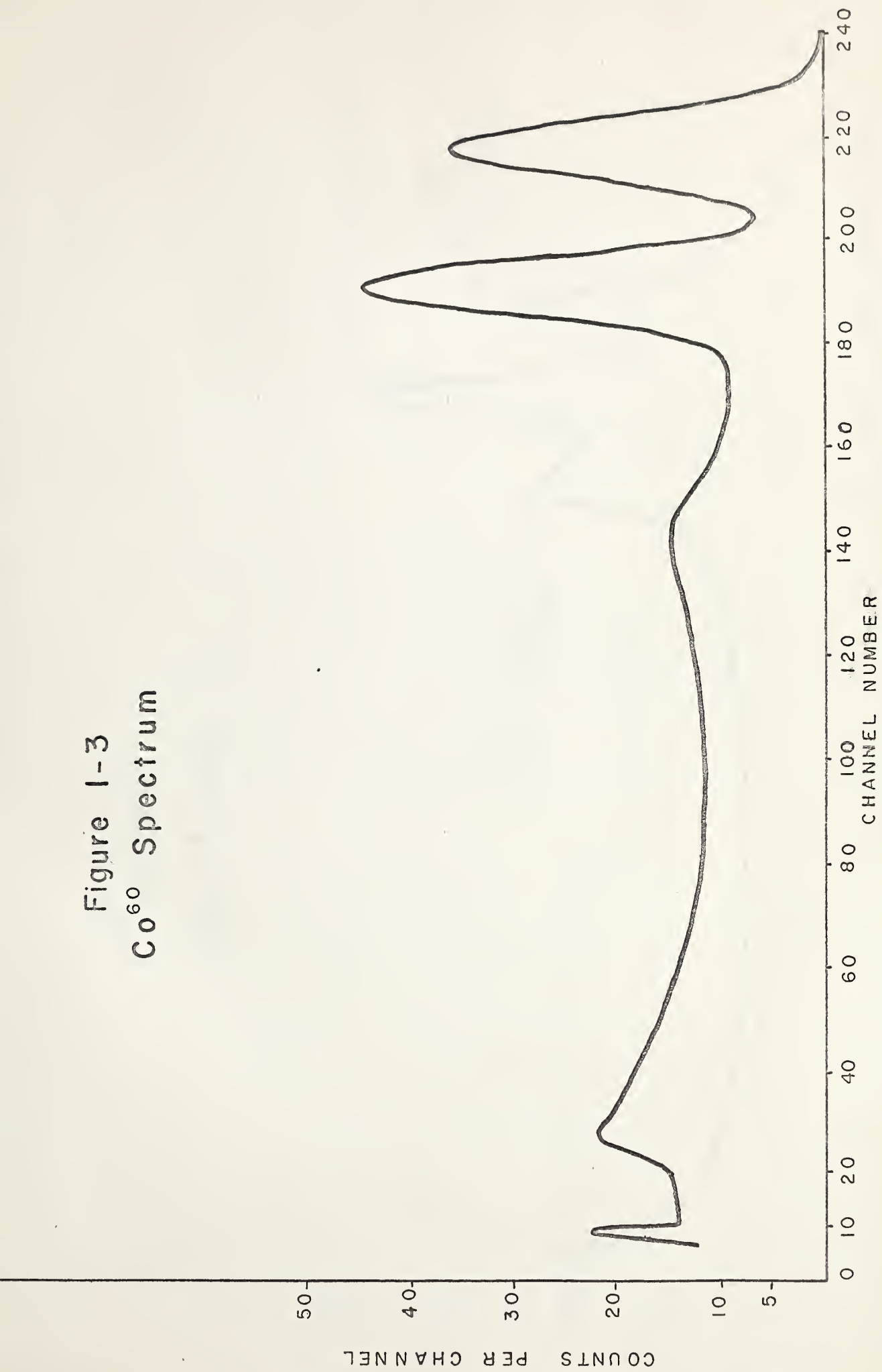
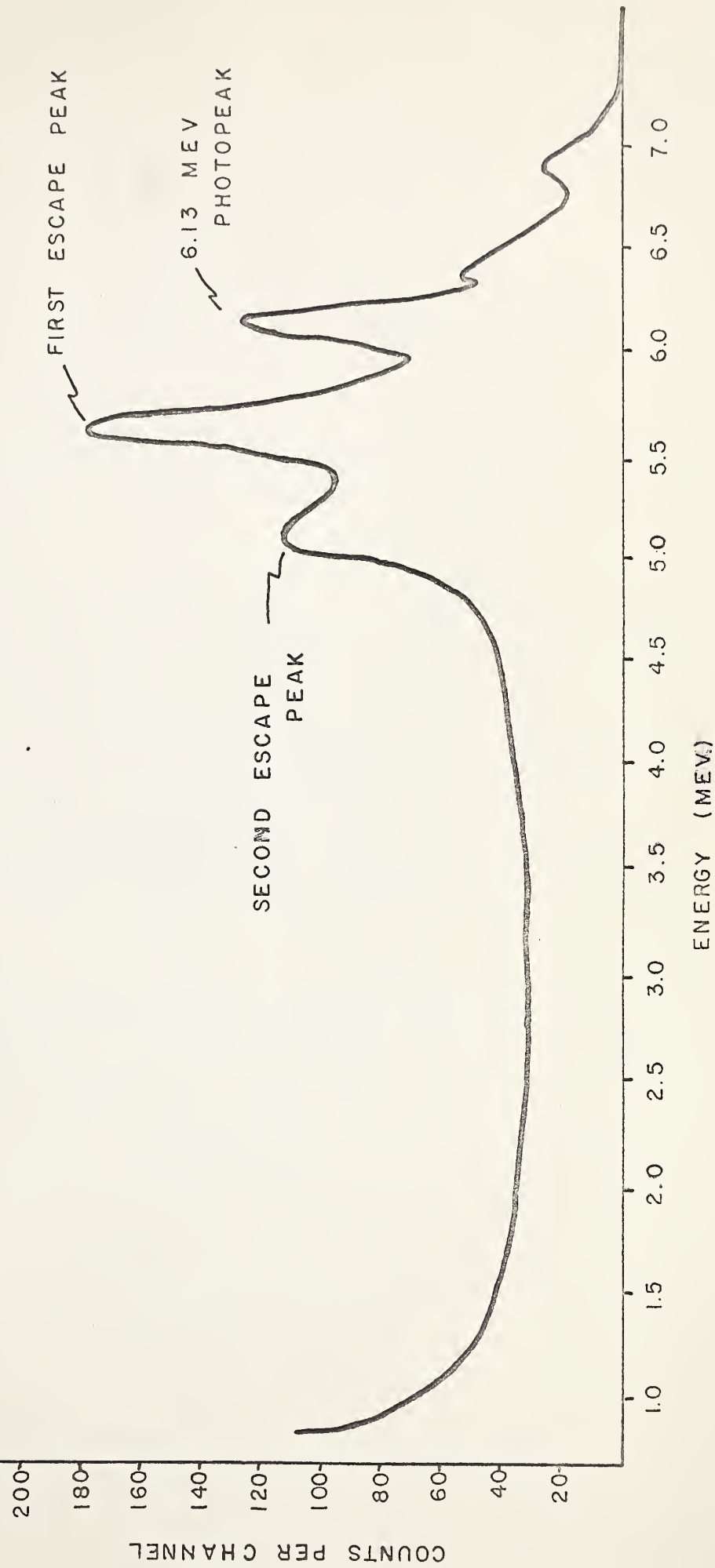


Figure 1-4
 $F^{19} (p, \alpha \gamma) O^{16}$

$E_p = 874 \text{ keV}$



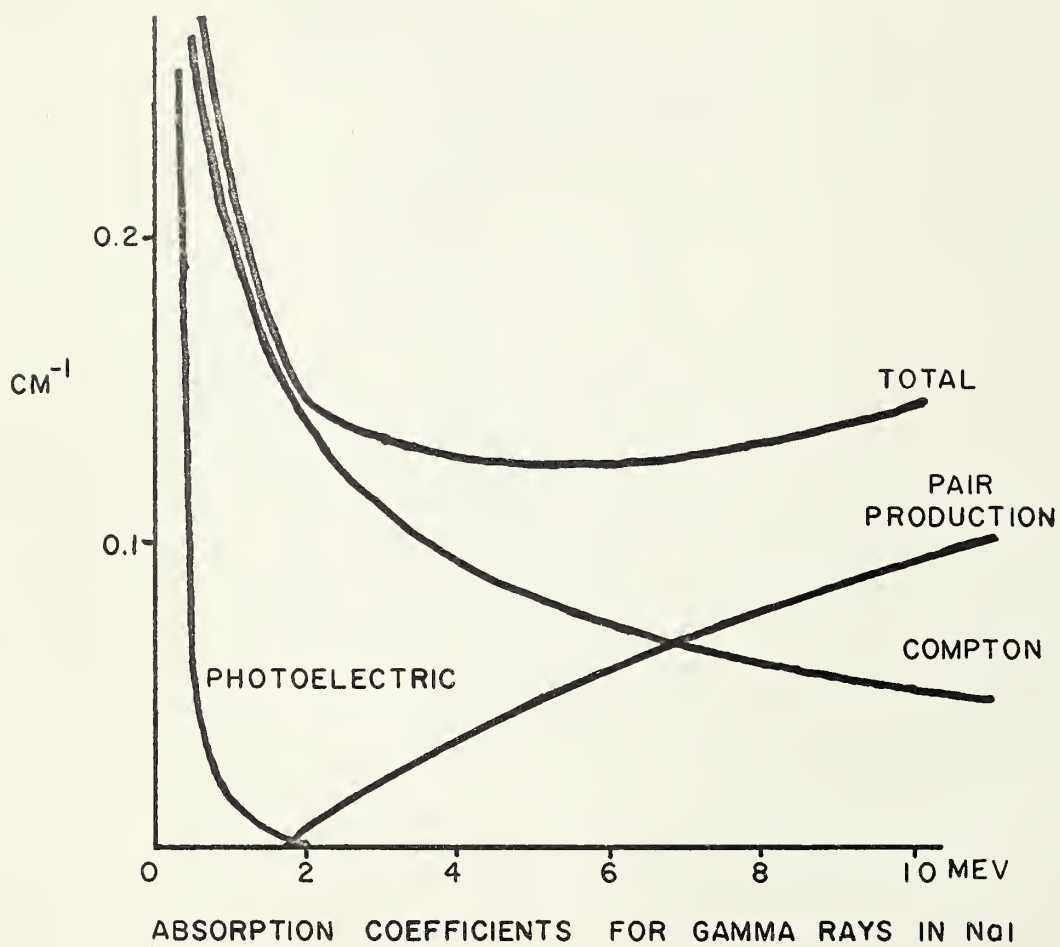


Figure 1-5

this experiment (0 - 8 MeV) the energy of a gamma ray is converted into electron energy through three processes which take place whenever gamma rays pass through matter.

1. Photoelectric Effect - the cross section is large at low energies, but approaches zero very quickly as the gamma ray energy approaches 1 MeV.

2. Compton Effect - the cross section is roughly constant at low energies, and slowly approaches zero in the region of 10 MeV to 100 MeV.

3. Pair Production - the cross section is zero below 1.02 MeV, but rises rapidly with increasing energy above this value.

Figure 1-5 exhibits the absorption coefficients in NaI for these three effects as a function of gamma ray energy.

It is possible that the total energy of an incident gamma ray may not be collected by the scintillation counter. This can arise for two main reasons.

1. A Compton scattered photon may escape from the scintillation crystal so that only a fraction of the incident gamma ray's energy is observed. This gives rise to a "Compton smear" of a relatively constant height terminating in a "Compton shoulder" a short distance below the photopeak (0.25 MeV for a high energy gamma ray) - see Figure 1-2. 0.25 MeV is the maximum energy which an electron can obtain in a Compton scattering event.

2. One or both of the 0.51 MeV gamma rays resulting from the annihilation of the positron produced in pair production may escape from the crystal. This gives rise to two "escape peaks" 0.51 MeV and 1.02 MeV below the photopeak. The size of the crystal detecting the incident gamma ray determines the relative sizes of the full energy photopeak and the two escape peaks. For the 3" x 3" scintillation crystal used in this experiment, the ratio of the heights of these peaks was 1 : 1.76 : 0.85 for the 6.13 MeV gamma ray from the reaction $F^{19}(p,\alpha\gamma)O^{16}$. That is, the most probable event was the escape of one of the 0.51 MeV annihilation gamma rays. This effect is exhibited in Figure 1-4.

General Description of Apparatus

In Figure 1-6 is shown a block diagram of the experimental apparatus. The photons from the sodium iodide scintillation crystal are transmitted to the photocathode of the Phillips 54AVP photomultiplier where they are converted to an electron pulse which is amplified by a factor of 10^6 . The output from the last dynode of the photomultiplier is then fed through a cathode follower to an amplifier where it is further amplified, the resulting signal being fed into a kicksorter and a discriminator. The discriminator in turn operates a scaler. The kicksorter used was a model CN110 256 channel Digital Computer Unit supplied by Technical Measurement Corp., North Haven Conn.

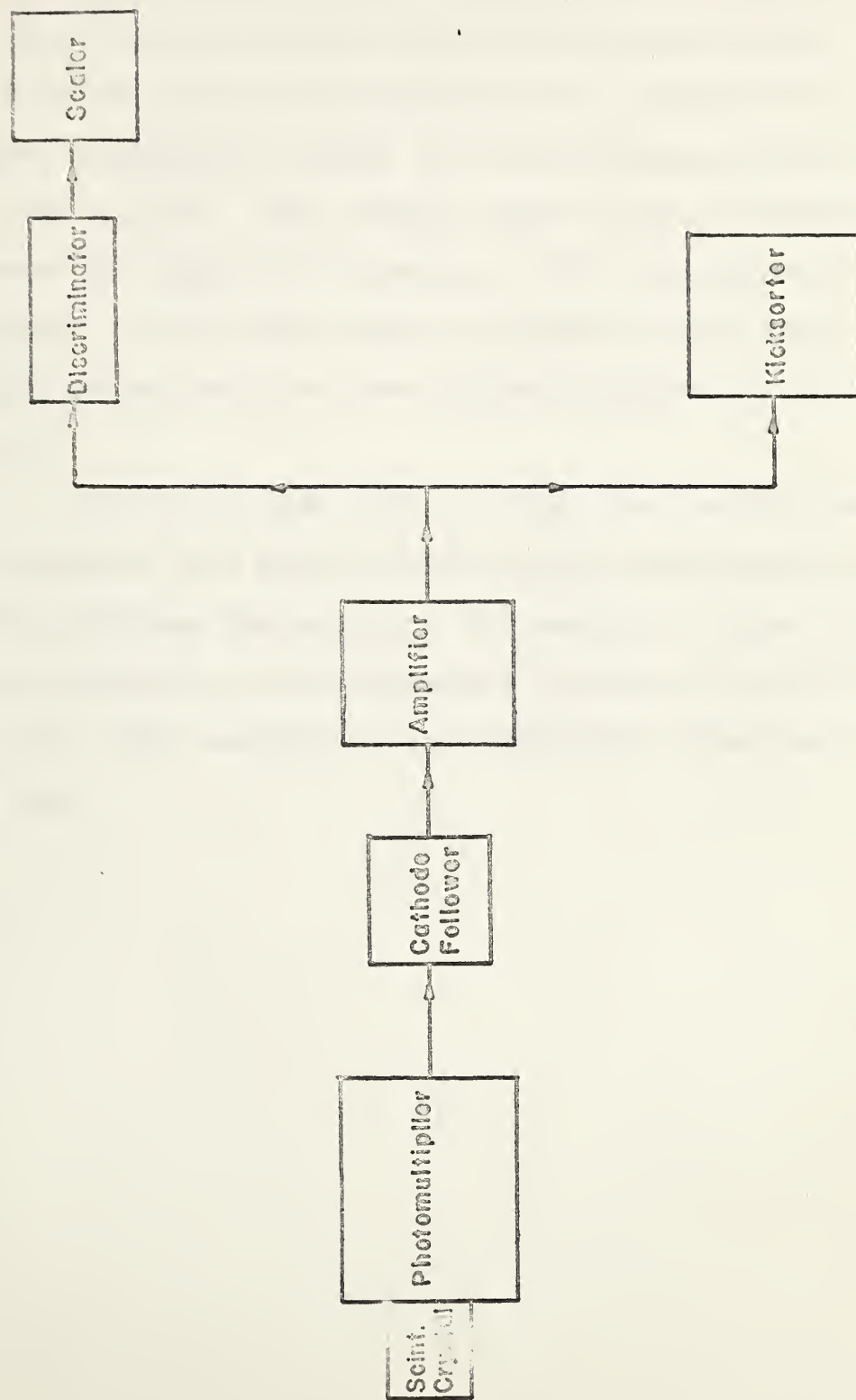
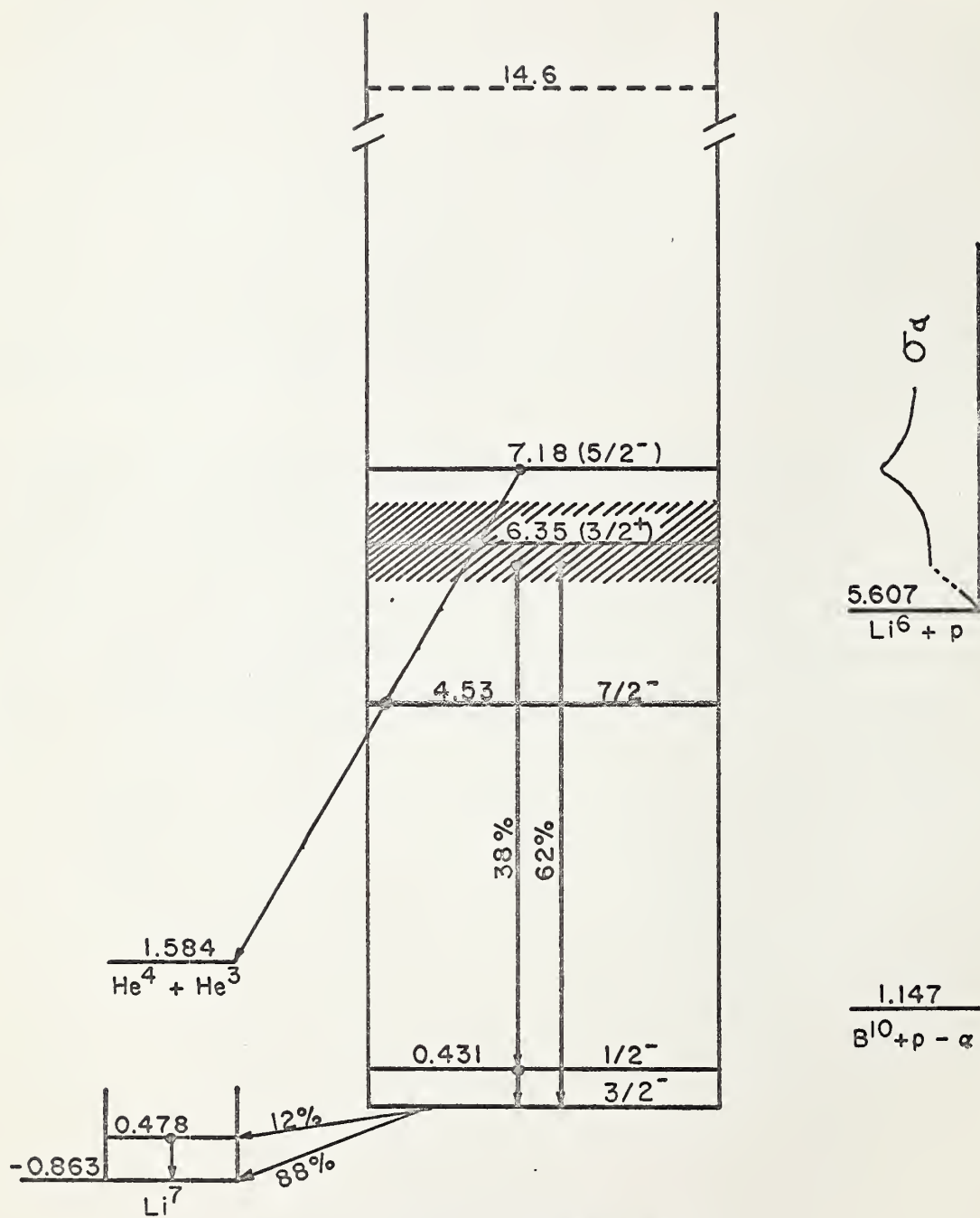


Figure 1-6

The gain of the amplifier was adjusted so as to place the $F^{19}(p,\gamma)O^{16}$ spectrum at the upper end of the kicksorter. The lower level and window width of the discriminator were then set so that the discriminator was triggered by all pulses equivalent to gamma rays with energies between 4.5 MeV and 6.3 MeV. This energy range of the discriminator covered the region of interest, so that the number of counts recorded by the scaler gave the yield of gamma rays in the energy range where the level under consideration was thought to lie.

The proton beam used to induce the desired reaction was provided by a type AK Positive Ion Accelerator supplied by High Voltage Engineering. The energy to which the protons were accelerated was continuously variable from 200 keV to 2.0 MeV. This energy was electronically stabilized to within ± 2 keV.



ENERGY LEVELS OF Be^7

Figure 2-1

SECTION 2. PREVIOUS WORK AND RESULTS

Previous Work

There has been a large amount of work done on the mirror nuclei Li^7 and Be^7 , but no attempt will be made to present a resume of all of it in this thesis - a complete discussion of the experimental work relating to Li^7 and Be^7 may be found in the compilation of Ajzenberg-Selove and Lauritsen (Aj59). Only that work will be discussed which deals directly with the reaction $\text{Li}^6(p, \gamma) \text{Be}^7$, or with the possible existence of an energy level between the 4.53 MeV and 6.35 MeV levels of Be^7 (or correspondingly the 4.63 MeV and 6.54 MeV levels of Li^7). Figure 2-1 shows the relevant level scheme for Be^7 (Aj59).

Stoll (St54), in studying the reaction $\text{Li}^7(\gamma, t) \text{He}^4$, reports the observation of three levels at energies of 4.7 MeV, 5.5 MeV, and 6.8 MeV when lithium loaded emulsions were bombarded with bremsstrahlung produced by a 31 BeV betatron. The relative intensities of the groups due to these levels are respectively 1 : 0.75 : 0.75. The 4.7 MeV and 6.8 MeV levels presumably correspond to the 4.63 MeV and 6.54 MeV levels in Li^7 , leaving the 5.5 MeV level unaccounted for.

Levinson and Banerjee in a paper entitled "Direct Interaction Theory of Inelastic Scattering" (Le57) give

spectra taken by Maxson and Bennett (Ma57), of protons inelastically scattered from Li^7 at three angles; 12° , 32° , and 60° . In the spectrum taken at 12° the evidence for a level at 5.5 MeV is as good as that for the levels at 6.6 MeV and 7.5 MeV, and although the evidence is not as strong at the other two angles shown, the possibility of a contribution from the 5.5 MeV level can not be ruled out.

In studying the reaction $\text{Li}^6(\text{p},\alpha)\text{He}^3$ Marion et al (Ma56) found resonance behaviour corresponding to the two states at 6.35 MeV and 7.18 MeV in Be^7 . In analyzing their data, however, it was noted that there was an unusually large non-resonant background. It is quite possible that this may indicate the presence of other states or perhaps some other form of direct interaction.

The above evidence would seem to indicate the presence of the state predicted by Chesterfield and Spicer, but other experiments do not confirm this. For instance, the results of searches for the 5.5 MeV level of Li^7 using the reactions $\text{Li}^6(\text{d},\text{p})\text{Li}^7$ and $\text{Be}^9(\text{d},\alpha)\text{Li}^7$ show no indication of such a level. In fact, from the d, α reaction, the intensity of the alpha group due to this level must be less than five percent of the intensity of the ground state alpha group or else the 5.5 MeV level would have been observed (Ge56).

Too much emphasis should not be placed upon the fact that the proton group arising from the 5.5 MeV level of Li^7 was not seen using the reaction $\text{Li}^6(\text{d},\text{p})\text{Li}^7$ since the group

due to the 6.54 MeV state was not observed either. The proton groups corresponding to the ground state, 478 keV level, and the 4.63 MeV level were, however, observed. The negative results in the case of this experiment could be interpreted as being caused by either a low cross section for this reaction or else by the broadness of the two levels (the 6.54 MeV level is known to have a width of approximately 1000 keV (Aj59)),

All other reactions which have been used to investigate the level structure of Li^7 and Be^7 show no indication of the level proposed by Chesterfield and Spicer.

Although there is admittedly a fair amount of negative evidence regarding a 5.5 MeV level in Li^7 , much of this is inconclusive. For instance; Erdos et al (Er54) have repeated the experiment of Stoll (St54) with better development techniques for the film, and have confirmed his finding of a 5.5 MeV level in Li^7 . After having done this they examined the negative results of all related experiments performed prior to 1954 and were able to show that these results are not in conflict with the existence of such a state.

It seemed that the information which was available relating to this level was such as to preclude a valid decision of any sort. For this reason it was decided to use the reaction $\text{Li}^6(p,\gamma)\text{Be}^7$ to search for any de-excitation gamma rays which might be emitted by the proposed level,

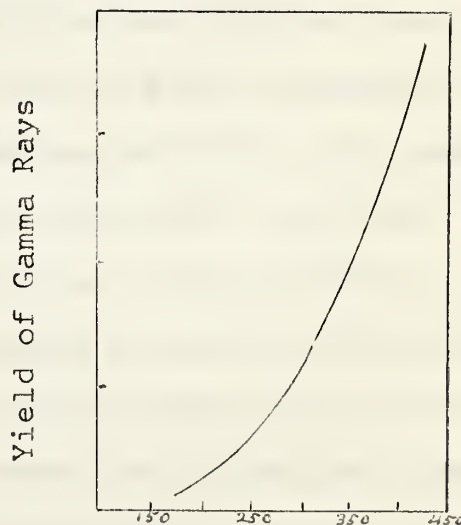
and also for any resonances in the gamma ray yield.

When Li^6 is bombarded with protons a large number of He^3 and alpha particles are observed, arising from the reaction $\text{Li}^6(p, \alpha)\text{He}^3$. This reaction exhibits two resonances, a broad one at about 1 MeV bombarding energy and another at 1.83 MeV (Ma56). In spite of the competition from this alpha process it has been possible to examine the capture gamma radiation from the reaction $\text{Li}^6(p, \gamma)\text{Be}^7$.

The first attempt to detect gamma rays from this reaction was unsuccessful, and an upper limit of 2.5×10^{-10} gammas per proton was deduced for 950 keV protons incident on a thick target (Cu39). Then, in 1954 a complicated pattern of de-excitation gamma rays was reported as having been observed at bombarding energies ranging from 400 keV to 2.2 MeV (Er54A). Shortly after

this Bashkin and Carlson (Ba55) determined that the cross section for the decay of the capture state through the 431 keV state was 0.06 $\mu\text{barns/steradian}$ at a bombarding energy of 415 keV.

In Figure 2-2 is shown the yield of 431 keV gamma rays for bombarding energies from 180 keV to 415 keV.



E_p in keV
Fig. 2-2

Gamma rays ranging in energy from 431 keV to $(5,60 \text{ MeV} + 6/7E_p)$ are possible when Li^6 is bombarded with protons whose laboratory energy is E_p . In addition to studying the gamma rays from cascades through the 431 keV level Bashkin and Carlson attempted to observe the gamma rays resulting from the decay of the broad 6,35 MeV level to the ground and first excited states of Be^7 . This was done at a bombarding energy $E_p = 300 \text{ keV}$, but due to the resolution of their detector the peaks were not resolved, and at energies above 340 keV they were obscured by the 6,13 MeV gamma rays from the $\text{F}^{19}(\text{p}, \alpha \gamma) \text{O}^{16}$ reaction in fluorine contamination.

Warren et al (Wa56) were able to observe the radiation from the de-excitation of the 6,35 MeV level of Be^7 in spite of fluorine contamination - this contamination spoiled the results only at the fluorine resonances and above $E_p \sim 1 \text{ MeV}$. In observing the radiation from the 6,35 MeV level they were able to determine that about 62% of the transitions go to the ground state. In conjunction with this they measured the cross section for the reaction $\text{Li}^6(\text{p}, \gamma) \text{Be}^7$ and found that it was $0,02 \text{ } \mu\text{barns/steradian}$ at $E_p = 750 \text{ keV}$ (about a factor of 10^5 smaller than the competing reaction $\text{Li}^6(\text{p}, \alpha) \text{He}^3$).

It is to be noted that the total cross section as determined by Warren et al is about a factor of 10 smaller than that which is obtained from the measurement of Bashkin and Carlson when the branching ratio between the ground and first

excited state is taken into account. One would normally expect that the cross section at $E_p = 415$ keV would be less than that at $E_p = 750$ keV. There seems to be two possible explanations for this; one, that Bashkin and Carlson were exciting some state other than, or in addition to, that at 6.35 MeV, and secondly that a small amount of contaminant such as B^{10} may have added greatly to the 431 keV radiation from the capture process. (Due to the smallness of the $Li^6(p,\gamma)Be^7$ cross section only a few parts per million of B^{10} would be necessary). In connection with this it is interesting to note that Warren et al observed an unusually large amount of 431 keV radiation arising from the reaction $B^{10}(p,\alpha)Be^7^*$ in boron contamination of their targets.

Experimental Results

The results which were obtained during the course of this experiment are exhibited in Figures 2-3 through 2-10. Figures 2-3a and 2-3b show the yield of gamma rays with energies between 4.5 MeV and 6.3 MeV measured as a function of the proton bombarding energy from 200 keV to 1.0 MeV. Whenever a new target was used, the resonances shown at 874 keV and 935 keV were run over so as to obtain a normalization factor on the amount of fluorine contamination on the target. (This was found to remain essentially constant). The proton bombarding energy was then lowered and a careful search made for any possible resonances in the gamma ray

Figure 2-3a
Gamma Ray Yield (90°)

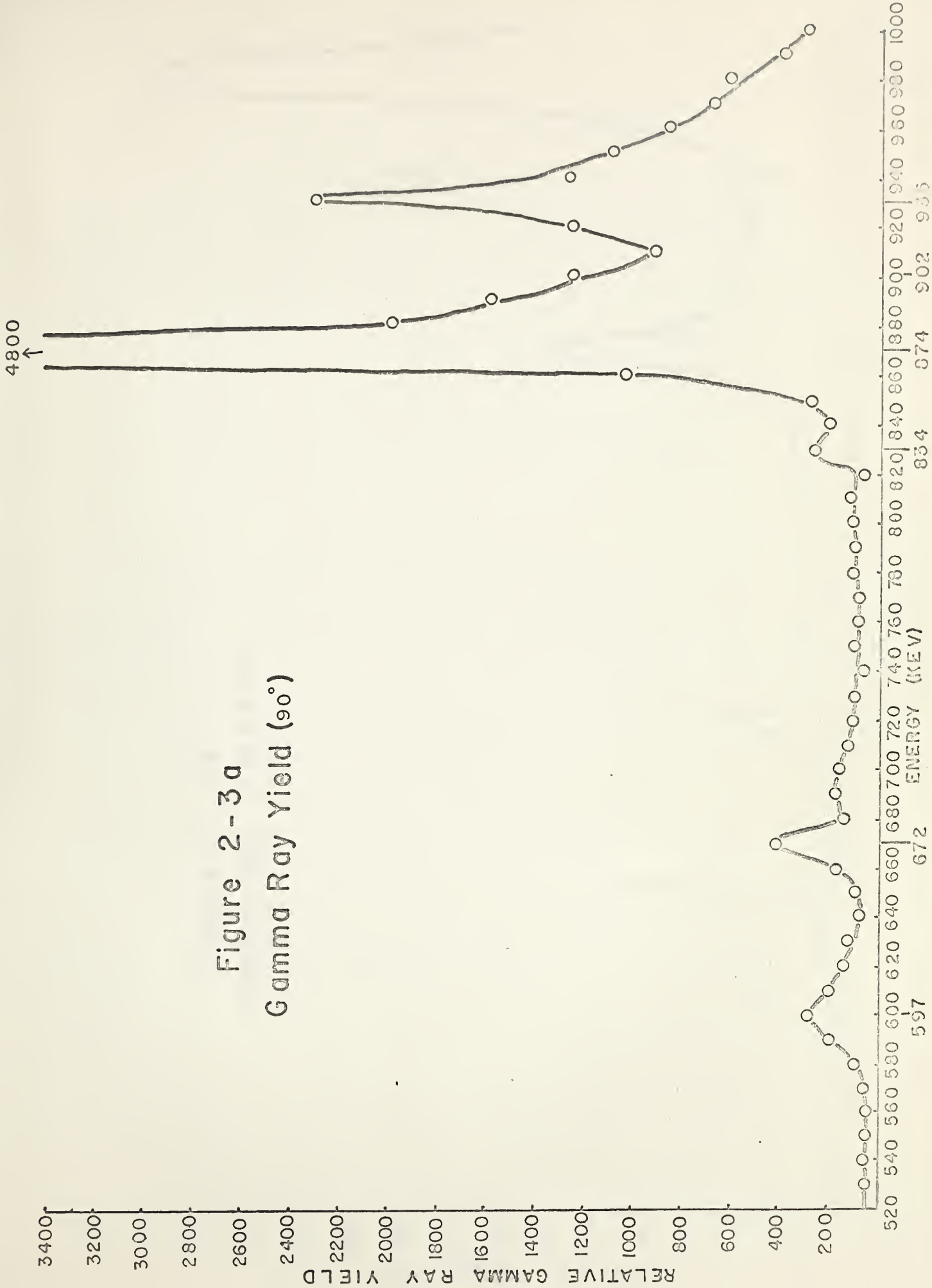
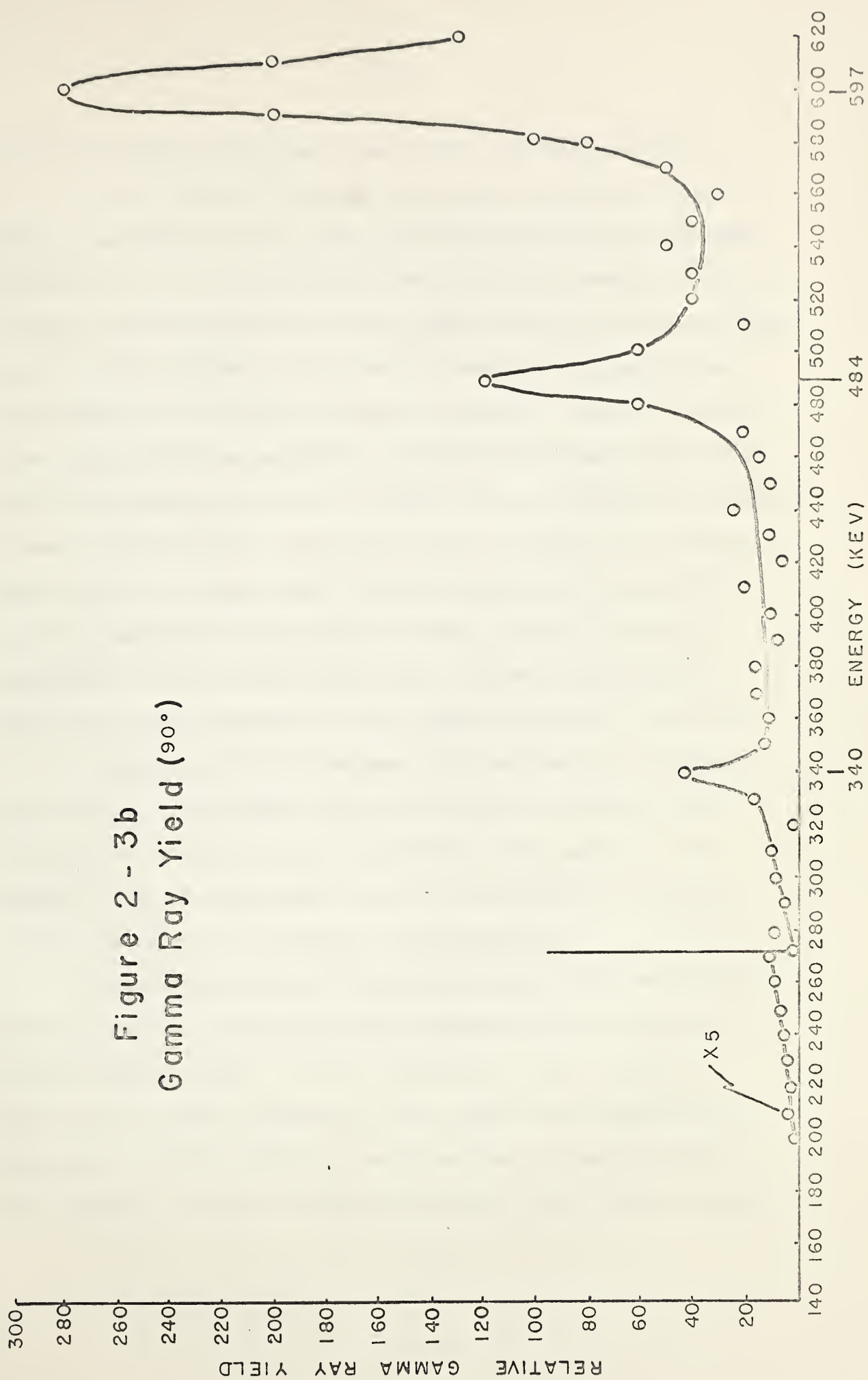


Figure 2 - 3b
Gamma Ray Yield (90°)



yield for proton energies between 200 keV and 450 keV.

In the range of proton bombarding energies between 200 keV and 300 keV the yield was measured for an incident charge of 1.5×10^{-4} coulombs, while for the energy range between 300 keV and 450 keV the gamma ray yield was measured for 3×10^{-5} coulombs. (It was not possible to normalize the amount of Li^6 on the various targets). As can be seen from Figure 2-3b no evidence of a resonance was found which would correspond to a level in Be^7 with an excitation energy between 5.88 MeV ($E_p = 200$ keV) and 6.14 MeV ($E_p = 450$ keV). This places an upper limit on the resonance cross section for the reaction $\text{Li}^6(p,\gamma)\text{Be}^7$ of about 5×10^{-3} $\mu\text{barns/steradian}$ in the region below $E_p = 330$ keV and about 1×10^{-2} $\mu\text{barns per steradian}$ in the region above $E_p = 350$ keV. If the level in Be^7 lies between the excitation energies 5.89 MeV ($E_p = 330$ keV) and 5.91 MeV ($E_p = 350$ keV) then it would be very difficult to detect it by means of the present type of experiment due to the radiation from the 340 keV resonance in fluorine contamination.

The yield curve of Figures 2-3a and 2-3b was taken at 90° to minimize the background radiation from the walls of the target room. It is no different from a similar yield curve which was taken at 55° where the angular distribution effects will be a minimum for the decay of the $3/2^-$ and $5/2^-$ levels to the ground and first excited state

of Be^7 since at this angle the $P_2(\cos \theta)$ term is equal to zero.

Figure 2-4 is the theoretical gamma ray spectrum expected from the reaction $\text{Li}^6(\text{p}, \gamma)\text{Be}^7$ for a proton bombarding energy of 800 keV. This spectrum has been calculated on the basis of the branching ratio of 66% to the ground state and 34% to the first excited state reported by Bashkin and Carlson (Ba55), and Warren et al (Wa56); and upon the line shape as determined from the observed shape of the 340 keV fluorine resonance spectrum. (This resonance has almost pure 6.13 MeV radiation). The experimental spectrum for this bombarding energy is shown in Figure 2-5. It will be noted that there are considerably more low energy counts than are predicted, a fact also noted by Warren et al.

A certain amount of low energy counts in excess of the number predicted for pure $\text{Li}^6(\text{p}, \gamma)\text{Be}^7$ radiation is expected since it is known that the contaminants C^{12} , O^{16} , and F^{19} are present in significant amounts. In addition to the gamma radiation from these contaminants, radiation from minute concentrations of other contaminants, not specifically detectable, will add to the general beam dependent background.

The peaks found at 5.25 MeV and 4.84 MeV of Figure 2-4 are too large by factors of 1.2 and 1.5 respectively. It is possible that this can be explained, in part at least,

Figure 2-4
Theoretical $\text{Li}^6(p,\gamma)\text{Be}^7$ Spectrum
for $E_p = 800 \text{ keV}$

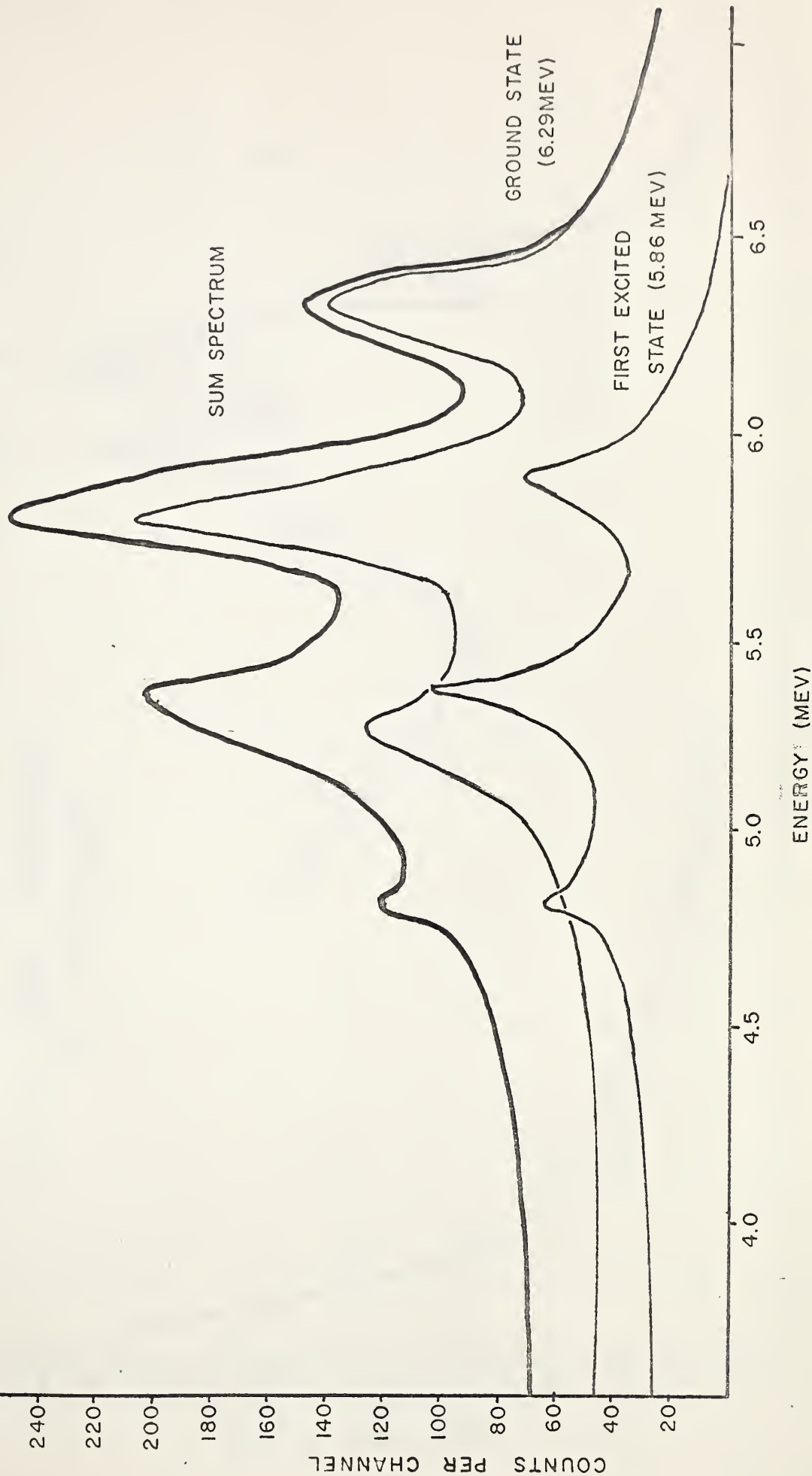
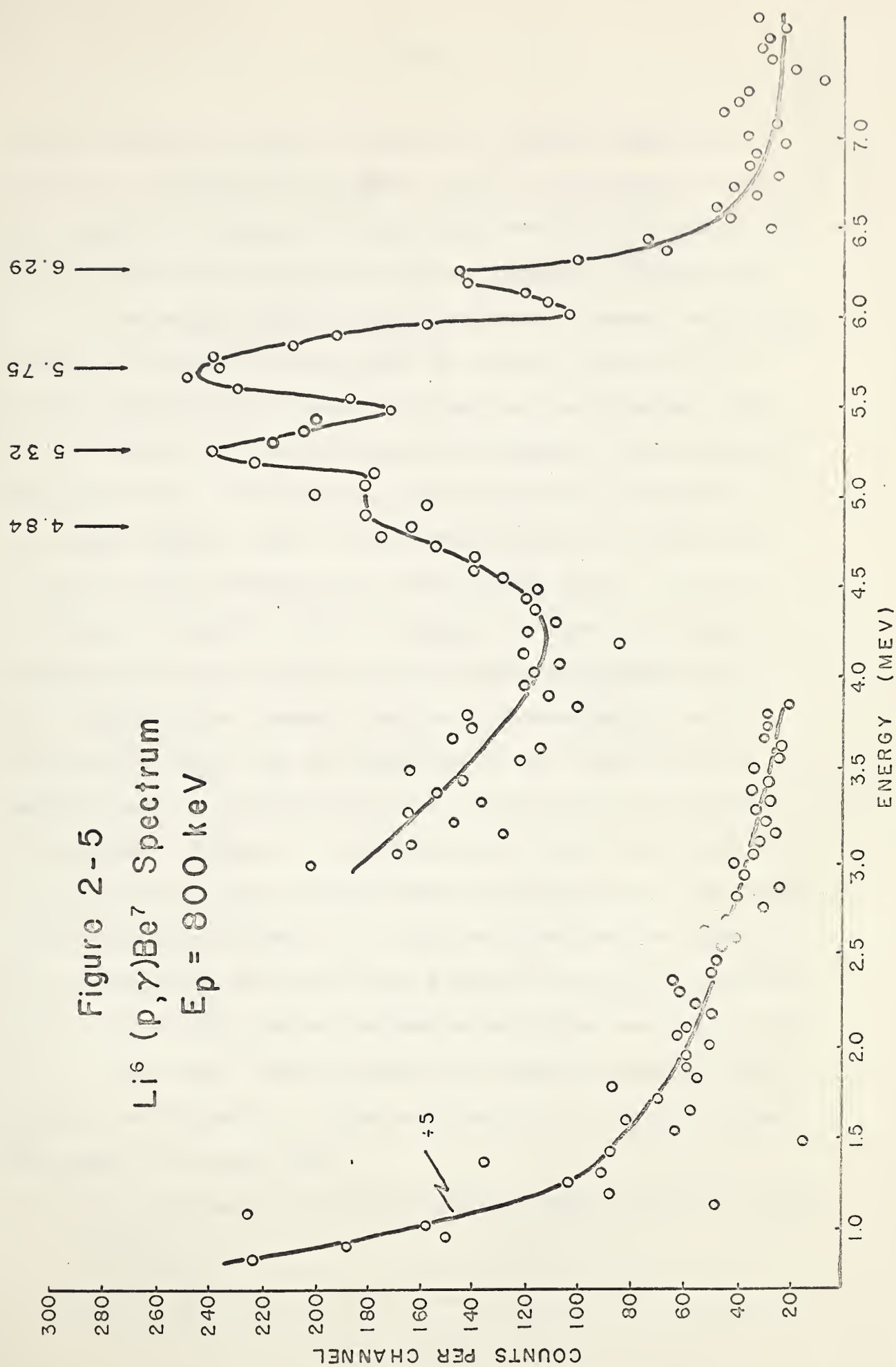


Figure 2-5
 $\text{Li}^6 (p, \gamma) \text{Be}^7$ Spectrum
 $E_p = 800 \text{ keV}$



by the presence of small amounts of fluorine radiation, since at a bombarding energy of 400 keV the radiation from the fluorine contamination and that from the broad 6.35 MeV level of Be^7 have roughly the same intensity (Figure 2-6).

The energy spectrum obtained with a proton bombarding energy of 300 keV is exhibited in Figures 2-7a and 2-7b before and after the background has been subtracted. The intensities of the various gamma ray peaks in this spectrum are not at all in agreement with that shown in Figure 2-4, the lower energy lines are much too intense in comparison with the full photopeak and first escape peak. It is not possible to explain this discrepancy in terms of fluorine radiation since, not only is the bombarding energy below the energy of the lowest fluorine resonance which was observed (340 keV), but the position of the first fluorine escape peak at 5.62 MeV falls in a trough of the observed $\text{Li}^6(p,\gamma)\text{Be}^7$ spectrum. The possibility that there might be a significant amount of nitrogen contamination on the target which was giving rise to the observed spectrum was checked by running over the relatively strong $\text{N}^{14}(p,\gamma)\text{O}^{15}$ resonance at $E_p = 1.06$ MeV, but no resonance behaviour could be found.

This would seem to leave two possible effects which could, individually or together, explain the observed spectrum shown in Figure 2-7b.

1. Radiation is being observed from some state in Be^7

Figure 2 - 6
 $\text{Li}^6(p,\gamma)\text{Be}^7$ Spectrum (90°)

$E_p = 400 \text{ keV}$

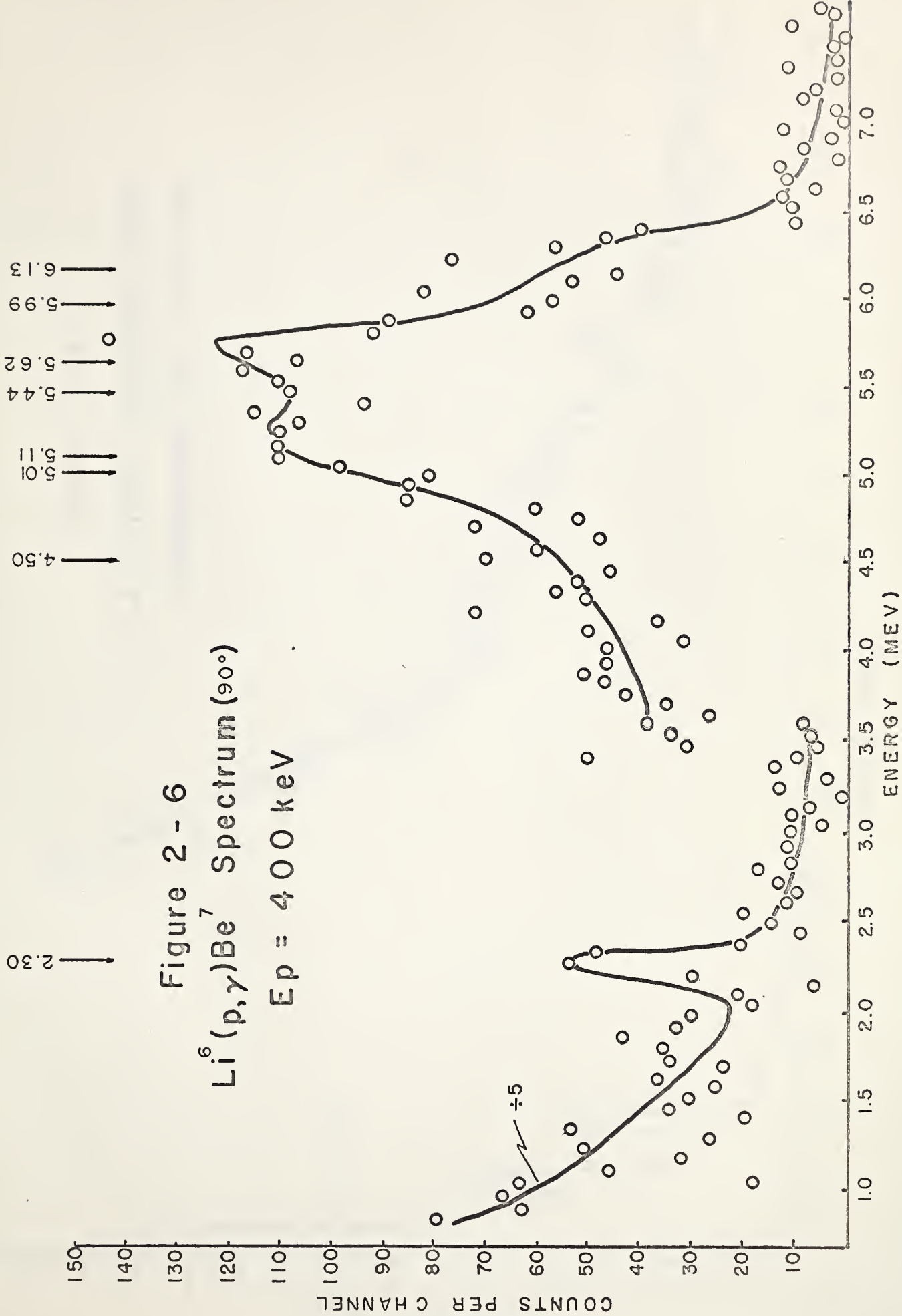


Figure 2-7a

$\text{Li}^6(\text{p},\gamma)\text{Be}^7$ Spectrum plus
Background. $E_p = 300 \text{ keV}$

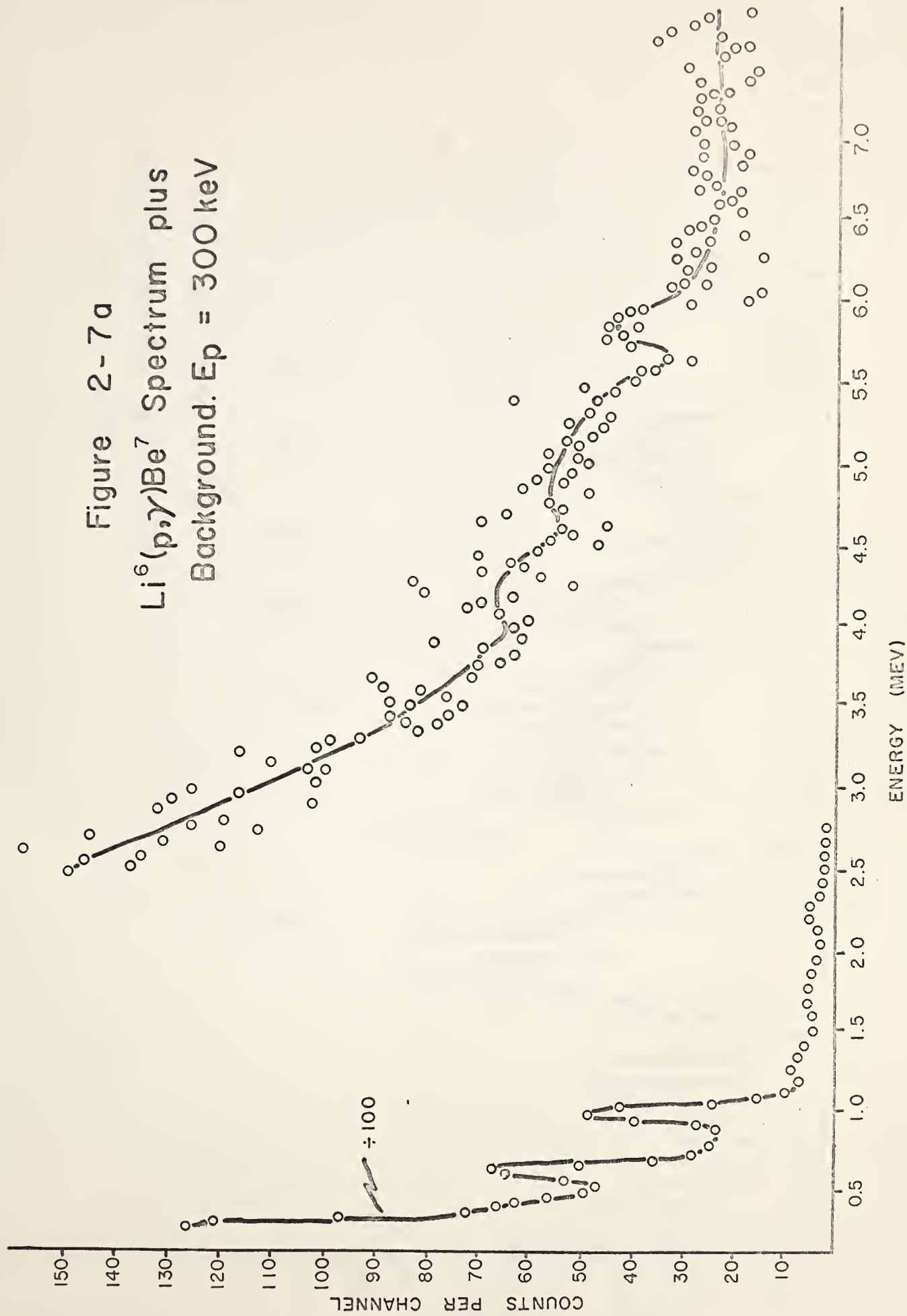
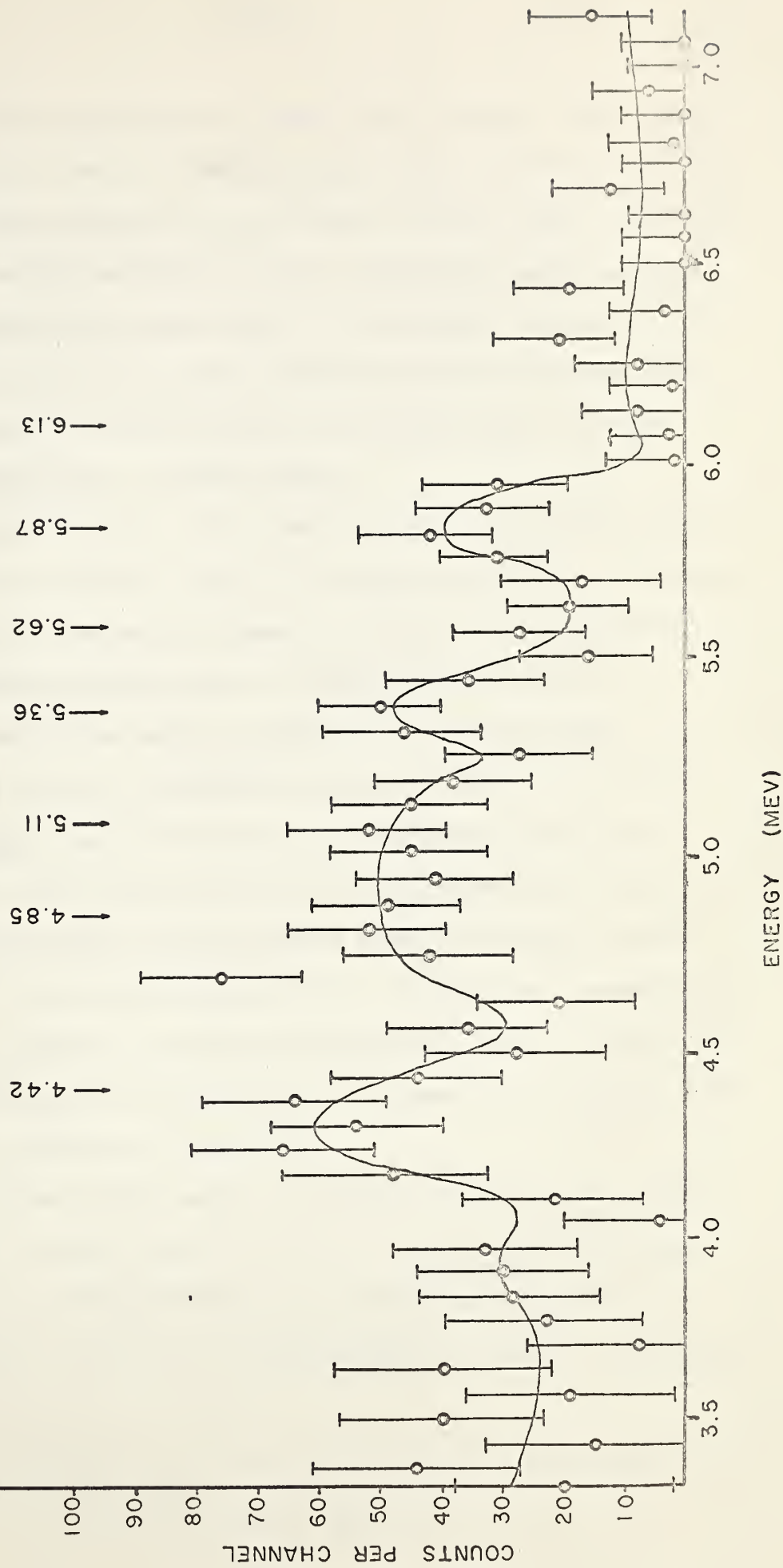


Figure 2-7b
 $\text{Li}^6(p,\gamma)\text{Be}^7$ Spectrum (90°)
 $E_p = 300 \text{ keV}$



other than, or in addition to, that at 6.35 MeV. This could be the 4.53 MeV level, or perhaps the level for which we are searching. The radiation from a state of Be^7 other than that at 6.35 MeV would presumably have a different decay pattern for the de-excitation gamma rays. A different value for the branching ratio to the ground and first excited states would be expected and, it is possible that there might even be cascades through the 4.53 MeV state.

2. The radiation from some contaminant on the target other than C^{12} , O^{16} , N^{14} , or F^{19} is being observed. However, no other single contaminant seems to be able to account for the intensities and positions of the observed peaks.

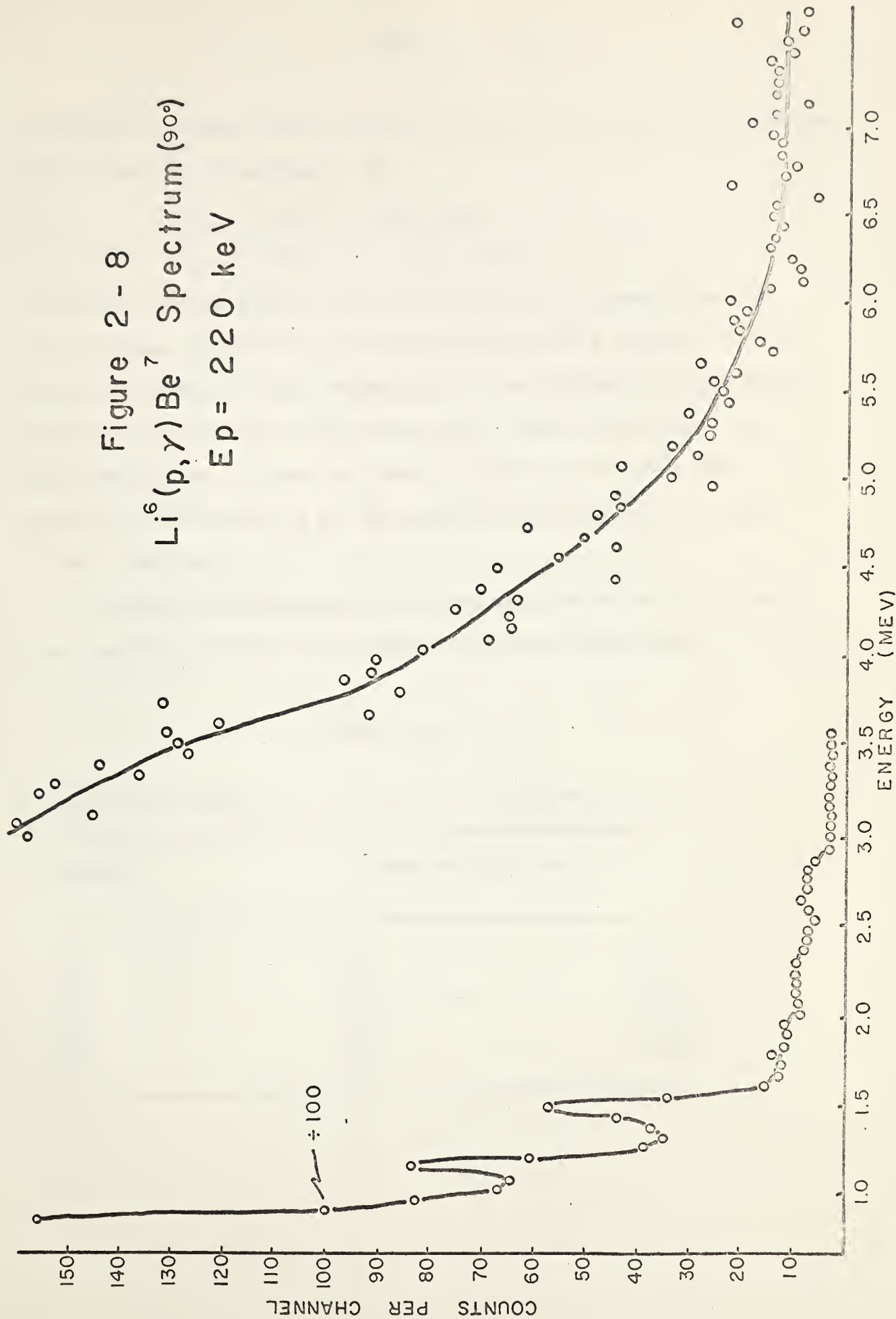
An attempt was made to observe the $\text{Li}^6(p,\gamma)\text{Be}^7$ reaction at a proton bombarding energy of 220 keV, but the number of counts was so low that no difference could be noted between this spectrum and the background spectrum even after the target had been bombarded with an incident charge of 9.5×10^{-4} coulombs (Figure 2-8). This is not unexpected since, on the basis of penetrabilities, the cross section for this reaction would be expected to decrease by a factor of 3 in going from 300 keV to 220 keV.

The ground state spin and parity of Li^6 is 1^+ , while that of the 6.35 MeV level of Be^7 is $5/2^-$ (according to the interpretation of Chesterfield and Spicer), therefore, in accordance with the laws of conservation of angular momentum

Figure 2 - 8

$\text{Li}^6(p, \gamma) \text{Be}^7$ Spectrum (90°)

$E_p = 220 \text{ keV}$



and parity we must have protons with an ℓ value which satisfies the following relations:

$$\pi_{6.5 \text{ Li}^6} (-1)^\ell = \pi_{6.35 \text{ Be}^7} ,$$

$$|\vec{1} + \vec{\ell} + \vec{1/2}| \geq I_{6.35 \text{ Be}^7} .$$

All odd ℓ values greater than 1 satisfy the above relations and are thus able to form the 6.35 MeV ($5/2^-$) state. If the spin and parity of this state is $3/2^+$ as listed by Ajzenberg-selove and Lauritsen (Aj59) then, in order to satisfy the above relations, ℓ must be even. Similarly to form the proposed $3/2^-$ level of Be^7 ℓ must be greater than or equal to one, and odd.

Table 2-1 tabulates the penetrabilities of $L = 0$ and $L = 1$ protons on Li^6 for a number of proton energies.

TABLE 2-1

Penetrabilities of $L = 0$ and $L = 1$ protons on Li^6

$E_p(\text{keV})$	Penetrability $\times 10^3$	
	$L = 0$	$L = 1$
800	295.	62.5
400	107.	12.5
300	66.6	6.24
250	41.6	2.94
220	26.3	2.00
200	19.2	1.25

An attempt was also made to observe the radiation from the broad 6.35 MeV level of Be^7 for proton energies above the 874 keV fluorine resonance, but the fluorine contamination was such that this was not possible. Figures 2-9 and 2-10 are respectively the spectra observed from the Li^6 target, and from the F^{19} target at a bombarding energy $E_p = 960$ keV. There is no significant difference in the shape of these two spectra.

Discussion

It would appear on the basis of a comparison of the spectra observed at $E_p = 400$ keV that the targets used in this experiment had considerably more fluorine contamination than did those of Warren et al. When this increased fluorine contamination is taken into account, the spectra taken at $E_p = 800$ keV are essentially in agreement; although the possibility that some other level of Be^7 or some additional contaminant reaction may be adding to the intensity of the peaks at 5.25 MeV and 4.84 MeV as observed in this experiment can not be completely ruled out.

In agreement with the results of Bashkin and Carlson exhibited in Figure 2-2, no evidence of a resonance in the $\text{Li}^6(p,\gamma)\text{Be}^7$ yield was found in the region $E_p = 200$ keV to $E_p = 450$ keV. However, it is still possible that such a level exists, provided that the state either has a low cross section for this reaction or else is a broad level which

Figure 2-9
 $\text{Li}^6(p,\gamma)\text{Be}^7$ Spectrum (90°)
 $E_p = 960 \text{ keV}$

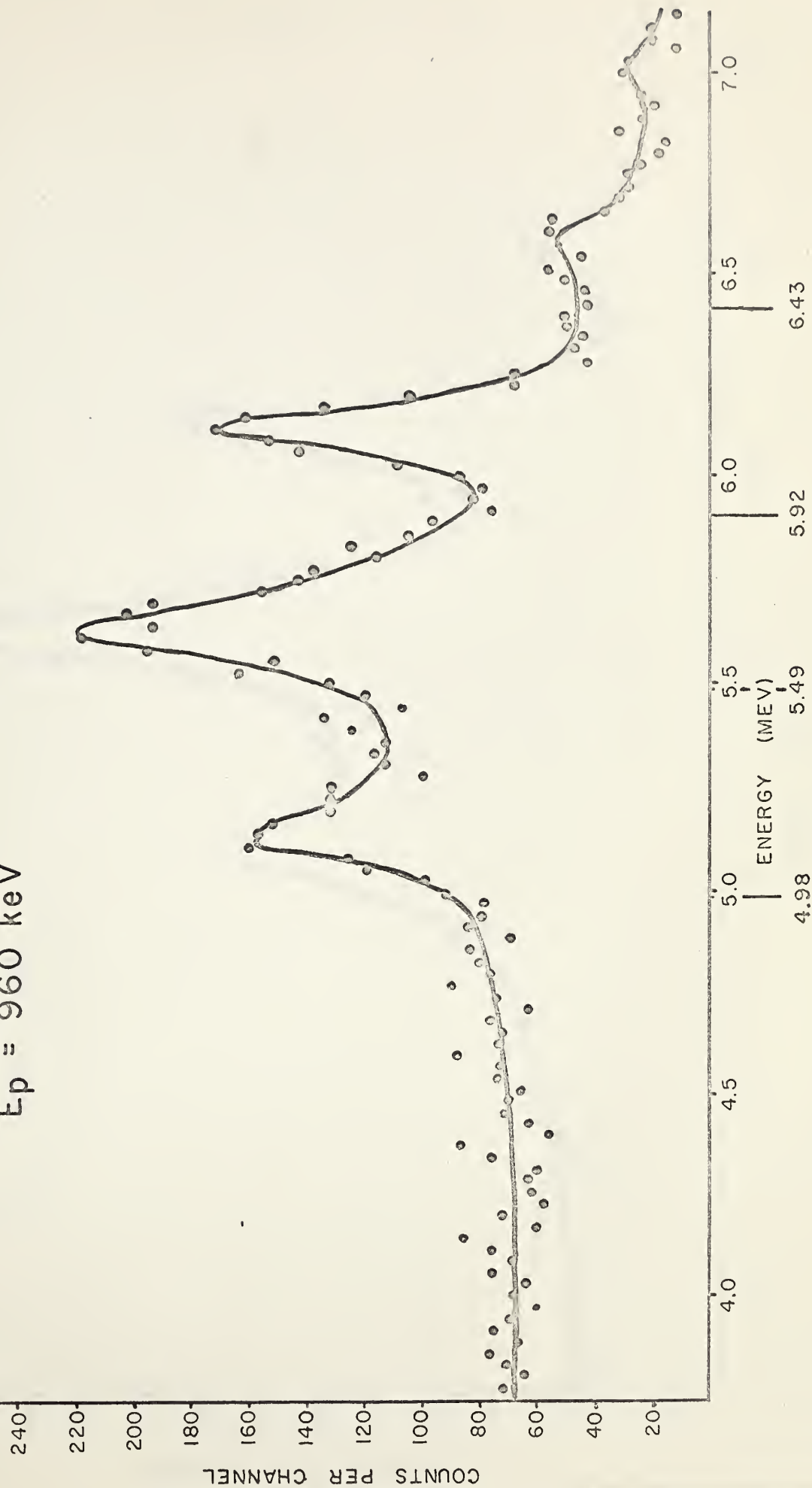
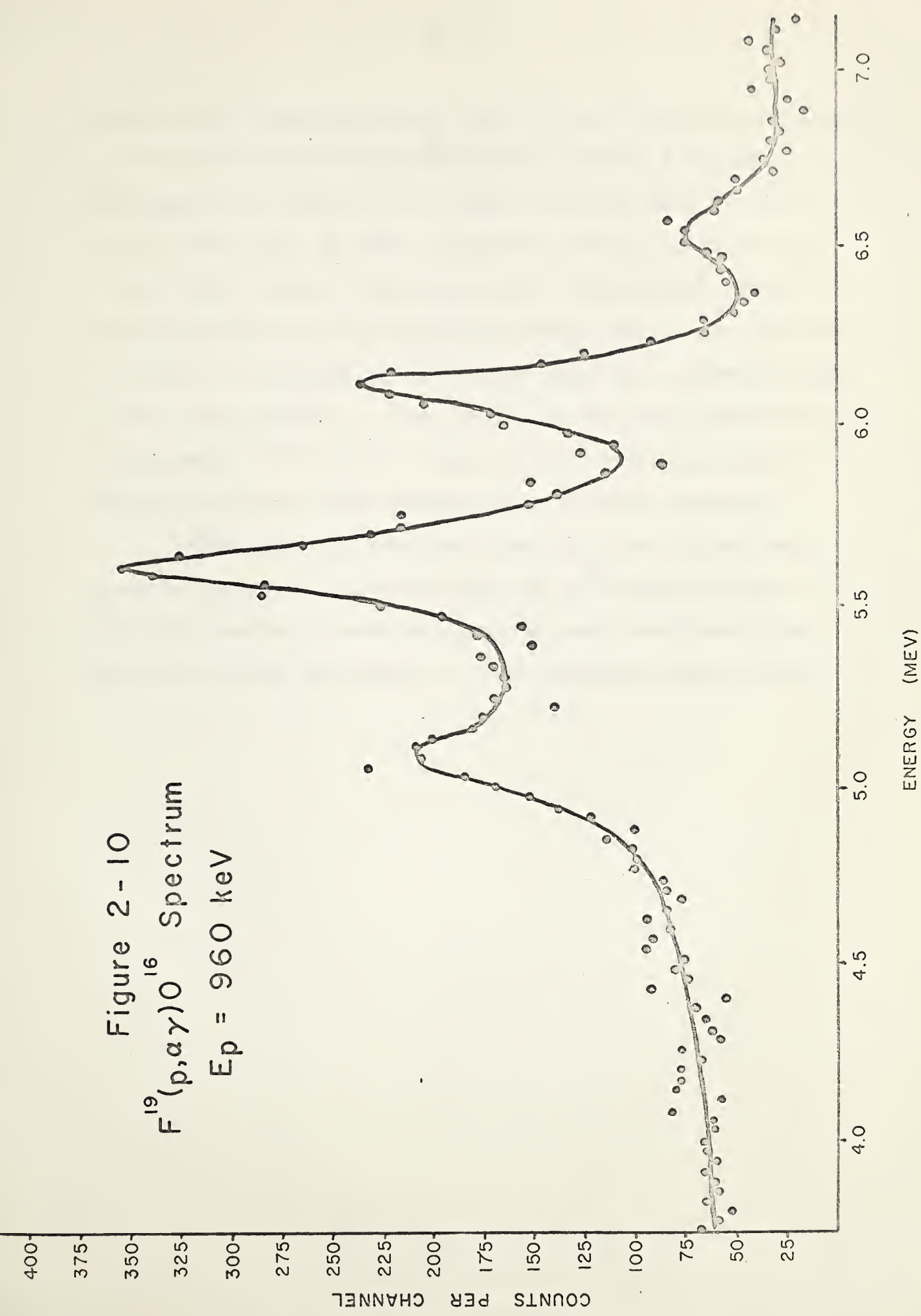


Figure 2-10
 $F^{19}(p,\alpha\gamma)O^{16}$ Spectrum
 $E_p = 960$ keV



merges with the known broad level at 6.35 MeV, as in neither case would it have been possible to observe a resonance in the gamma ray yield. It is quite probable that if the proposed level lies in this excitation region, it will have a large cross section for decay into a He^3 and He^4 particle, since for the 6.35 MeV level the cross section for this mode of decay is a factor of 10^5 larger than the competing gamma decay cross section. Also, so far as has been determined by experiment, the 4.53 MeV state decays almost completely by breaking up into a He^3 particle and an alpha particle.

The gamma-ray spectrum taken at $E_p = 300$ keV would seem to indicate that some state of Be^7 other than that at 6.35 MeV was being excited, however more experimentation must be carried out before a final judgement can be made.

SECTION 3. THE ROTATIONAL MODEL

The basic premise upon which the "nuclear shell model" is based is that the constituent nucleons move in a spherically symmetric binding field, representing the average effect of all interactions between nucleons. This model has been very successful in explaining a number of the properties of nuclei. For example: (i) magic number discontinuities in binding energies, (ii) beta-decay systematics, and alpha-decay systematics, (iii) islands of isomerism, (iv) orders of magnitude of magnetic moments of odd A nuclei. In addition to this, it has also been quite successful in predicting the nuclear ground state spins and parities.

The description of a nuclear state, in which one considers the independent motion of nucleons in a spherically symmetric potential well (the independent particle approximation) is, for many purposes, a rather good approximation in the case of closed shell configurations. However, for nuclear configurations with several particles outside of a closed shell, it is necessary to consider, also, that part of the nucleonic interactions which are not contained in the average field. This arises due to the fact that the solutions in the independent particle approximation are degenerate, and hence

even relatively small residual interactions among nucleons can introduce important correlations in the motion of the particles outside of the closed shell. For configurations with only a few particles outside of a closed shell one may attempt to treat the correlations by considering in detail the coupling in the motion of these few nucleons. However, a detailed treatment along these lines becomes very complicated if the number of particles is not very small. Thus, in addition to the coupling between the angular momentum of the particles, it is often necessary to include configuration mixing and interaction with closed shells.

One of the main difficulties with the usual independent particle model is that it is unable to predict the existence of very large electric quadrupole moments and very fast electric quadrupole gamma-ray transitions. The experimental quadrupole moments are as much as thirty times as large as those expected on the basis of this model, and a large number of E2 transitions in the rare earth region of the periodic table are enhanced by more than a factor of one hundred. On the basis of configuration interactions it would be necessary to have a strong constructive interference between the component electric quadrupole amplitudes in order to obtain such a large total amplitude. This is, in effect, a definition of collective motion, i.e., the only way in which one can obtain a large quadrupole effect is if many charged particles are participating in collective motion.

In spite of this apparent complexity, one finds that the energy spectra of nuclei with many particles outside of a closed shell exhibit a number of very simple features, which vary in a systematic way from nucleus to nucleus. These regularities are associated with the fact that a large part of the correlations between the particles can be described in terms of ordered collective motion of the nucleons, corresponding to simple variations in the nuclear shape. One is thus led to a generalization of the "shell model" in which the binding field is no longer assumed to be a static isotropic potential, but rather a slowly varying, non-spherically symmetric field. The introduction of such a field means that the nuclear shape and orientation must be considered to be dynamical variables. These variables are associated with the collective types of nuclear motion which accompany variations in the binding field. The interplay between these collective modes of motion, and the individual particle motion forms the basis of the "unified nuclear model".

The first problem which must be solved is the determination of the nuclear equilibrium shape. If the nucleus had an amorphous structure like a liquid drop, the spherical state would have the lowest energy, but the shell structure implies a tendency for distortions of the nuclear shape since the orbits of individual particles are strongly anisotropic. A simple description of this deformation effect was first given

by Rainwater (Ra50). According to this description a nucleon moving in a nuclear potential with a deformable surface exerts a centrifugal pressure which tends to produce an oblate deformation of the nuclear surface. In closed shell configurations, the nucleonic orbits are orientated equally in all directions so that the nucleus will have a spherical equilibrium shape, but particles in unfilled shells will tend to deform this shape.

The variable anisotropic binding potential includes a large portion of the nucleonic interactions in the average field, but significant residual interactions between particles remain (those interactions which can not be considered part of the average binding field of the nucleus), to give rise to the characteristic differences in binding energies of even-even, odd-A, and odd-odd nuclei (the pairing effects). These pairing forces tend to couple two equivalent nucleons together to form a state of zero total angular momentum, i.e. a spherically symmetric state. The pairing forces then, to some extent, counteract the tendency of individual nucleons to deform the nuclear shape. The nuclear equilibrium shape and the character of the collective modes of motion can be understood in terms of the competition between these two effects - the deforming power of the individual nucleons and the effect of the pairing forces.

In the region of the closed shells, the pairing effects dominate so that the nuclear equilibrium shape is spherical and the individual particle spectrum may be obtained by

considering particle motion in a spherical field as in the "shell model". It is to be expected, however, that in these regions the nuclei will also have modes of excitation corresponding to collective vibrations about the equilibrium shape.

The addition of particles leads to the nucleus becoming softer against deformations (Ra57). This softening manifests itself as a decrease in the frequency for collective vibrations about the spherical equilibrium state. For sufficiently many particles outside of a closed shell, the spherical shape becomes unstable and the nucleus acquires an ellipsoidal equilibrium shape (Mo57). For such nuclei the collective motion separates into rotational and vibrational modes. The former correspond to rotations of the nuclear orientation with the preservation of shape, and possess very low excitation energies, while the latter correspond to oscillations about the anisotropic equilibrium shape. It is to be expected, of course, that for certain nuclei the coupling between the collective and intrinsic modes (those degrees of freedom which correspond to the excitation of individual nucleons rather than the nucleus as a whole), or between the various collective modes of motion, will be such as to give rise to a very complicated structure of nuclear states.

In what follows we will be dealing with the "rotational model", a special form of the "unified model". That is, it will be assumed that the nuclei are non-spherical but

essentially spheroidal, and in addition that the nuclear motion separates into intrinsic and rotational modes. (For the purpose of this discussion the vibrational modes are included in the intrinsic mode classification).

The collective rotation of an axially symmetric nucleus has a number of similarities with the rotation of a symmetric top, and for this reason we will consider briefly the motion of a symmetric top. Let us denote a set of mutually perpendicular axis which are fixed in the rotating body as the 1, 2, 3 axes, the last of which is to be taken along the symmetry axis. The orientation of this body fixed set of axes is specified by three Euler angles α , β , γ . Because of the axial symmetry of the top, two of the principal moments of inertia are equal. The Hamiltonian of the system is then given by:

$$H_{\text{sym. top}} = \sum_{\nu=1}^3 \frac{\hbar^2}{2\mathcal{I}_\nu} R_\nu^2 = \frac{\hbar^2}{2\mathcal{I}} (R^2 - R_3^2) + \frac{\hbar^2}{2\mathcal{I}_3} R_3^2, \quad (1)$$

where \mathcal{I}_3 and \mathcal{I} denote respectively the moments of inertia for rotations about the symmetry axis and about an axis perpendicular to the symmetry axis and the R_ν denote the components of angular momentum along the corresponding body fixed axes.

The eigenfunctions of the symmetric top are the well known \mathcal{D} functions†. The action of the angular momentum

† The \mathcal{D} functions can be considered to be either the transformation functions for spherical harmonics under finite rotations, or the irreducible representations of the $2L + 1$ dimensional rotation group. We thus have:

$$Y_{LM}(\theta, \phi) = \sum_{M'} Y_{LM'} \mathcal{D}_{MM'}^L(\alpha, \beta, \gamma),$$

and

$$\mathcal{D}_{MM'}^L(\alpha, \beta, \gamma) = e^{iM\alpha} \mathcal{H}_{MM}^L(\beta) e^{iM'\gamma},$$

where the $\mathcal{H}_{MM'}^L$ are Jacobi polynomials.

operators upon these \mathcal{D} functions can be expressed as follows:

$$\begin{aligned} I_2 \mathcal{D}_{MK}^I &= M \mathcal{D}_{MK}^I, \\ I_3 \mathcal{D}_{MK}^I &= K \mathcal{D}_{MK}^I, \\ I^2 \mathcal{D}_{MK}^I &= I(I+1) \mathcal{D}_{MK}^I. \end{aligned} \quad (2)$$

Thus the solutions correspond to a total angular momentum I , angular momentum M along the z axis, and angular momentum K along the 3 axis (we must of course have $|K|$ and $|M| \leq I$).

The rotational motion of a nucleus differs from that of a symmetric top in one very important respect, namely; we must treat explicitly the degrees of freedom associated with excitations of the loosely bound nucleons, e.g. the unpaired nucleon in an odd- A nucleus. The intrinsic wavefunction (i.e. the wavefunction which is obtained when one assumed a static, spherically symmetric binding potential), is not an eigenfunction of the total intrinsic angular momentum j since the actual potential is spheroidal and slowly varying. However, since the potential is axially symmetric, the 3-component of the intrinsic angular momentum will be a constant of the motion which we will denote by Ω . We will now designate the intrinsic wavefunction by χ_τ where τ refers to all of the quantum numbers which are needed in addition to Ω to characterize the intrinsic state. This wavefunction is, of course, a function only of the particle co-ordinates in the body fixed system.

We now divide the total angular momentum of the system (\vec{I}) up into intrinsic and rotational parts, \vec{j} and $\vec{R} = \vec{I} - \vec{j}$ respectively. The nuclear Hamiltonian can then be expressed as:

$$H \doteq H_{\text{int}}(\vec{R}') + T_{\text{rot}} \quad , \quad (3)$$

where $H_{\text{int}}(\vec{R}') = \frac{p'^2}{2m} + V(\vec{R}')$,

and by analogy with (1)

$$T_{\text{rot}} = \sum_{\nu} \frac{\hbar^2}{2I_{\nu}} (I_{\nu} - j_{\nu})^2 = \frac{\hbar^2}{2J} [(\vec{I} - \vec{j})^2 - (I_3 - j_3)^2] + \frac{\hbar^2}{2J_3} (I_3 - j_3)^2 \quad . \quad (4)$$

In the above, T_{rot} is the total kinetic energy associated with the rotational motion.

We can now expand the above by expressing T_{rot} as the sum of two terms:

$$T_{\text{rot}} = T_{\text{rot}}^{\circ} + T_{\text{coupl.}} \quad , \quad (5)$$

where $T_{\text{rot}}^{\circ} = \frac{\hbar^2}{2J} [(\vec{I}^2 - \vec{j}^2) - (I_3 - j_3)^2] + \frac{\hbar^2}{2J_3} (I_3 - j_3)^2$,

and $T_{\text{coupl.}} = - \frac{\hbar^2}{2J} [2\vec{I} \cdot \vec{j}]$.

T_{rot}° can be thought of as an ordinary rotational term in that it is diagonal in both the $\chi_{\vec{R}}$ and \mathcal{D}_{MK}^{\pm} representations. $T_{\text{coupl.}}$ is the sum of a diagonal and a non-diagonal element, and will be expressed as such:

$$T_{\text{coupl.}} = - \frac{\hbar^2}{2J} I_3 j_3 - \text{R.P.C.} \quad , \quad (6)$$

where R.P.C. is what is usually defined to be the rotation particle coupling. If the particle is tightly bound to the

rotor, i.e. if the energy splittings of H_{int} are large with respect to the rotational energies, then the off diagonal matrix elements of R.P.C. can be neglected as small perturbations.

The above expression for the nuclear Hamiltonian can be further simplified if we recall that an axially symmetric equilibrium shape has been assumed. If such is the case, it is then impossible to distinguish orientations of the nucleus which differ only by a rotation about the symmetry axis, and this means that we must have $R_3 = 0$. With this simplification we have:

$$T_{rot} = \frac{\hbar^2}{2I} (\vec{I}^2 - J^2). \quad (7)$$

so that the nuclear Hamiltonian can be expressed as:

$$H = H_{int}(\vec{R}) + \frac{\hbar^2}{2I} [(\vec{I}^2 - J^2) - 2I_3 J_3] \quad (8)$$

A normalized eigenfunction of this Hamiltonian is:

$$\Psi = \left(\frac{2I+1}{2\pi^2} \right)^{1/2} \chi_{\Omega}^T D_{MK}^I(\alpha, \beta, \gamma).$$

This wavefunction must be refined to take into account the assumed symmetry properties of the nuclear shape. The existence of axial symmetry, which was used to simplify the nuclear Hamiltonian, implies that the nuclear wavefunction must be invariant with respect to an arbitrary rotation of the body-fixed reference frame about the symmetry axis. Such a rotation through an angle ϕ has the effect of transforming the Euler angles α, β, γ into $\alpha, \beta, \gamma + \phi$ so that

$$\mathcal{D}_{MK}^I \rightarrow e^{iK\psi} \mathcal{D}_{MK}^I,$$

and $\chi_{\Omega}^{\tau} \rightarrow e^{-i\Omega\psi} \chi_{\Omega}^{\tau}.$

The exponents in the above two equations have opposite signs since the \mathcal{D} function is the wavefunction of the body system with respect to the laboratory system, while the intrinsic function is the wavefunction with respect to the body system. For the nuclear wavefunction to be invariant we clearly must have:

$$e^{i(K-\Omega)\psi} = 1,$$

or $K = \Omega.$

A spheroid has another important symmetry property which must be induced onto the nuclear wavefunction. This property is its invariance with respect to rotations of 180° about any axis going through its center. Let us consider a rotation of 180° about the 1-axis (x' -axis) - this transforms the Euler angles α, β, γ into $\pi+\alpha, \pi-\beta, \gamma$, and results in the following transformations of the \mathcal{D} functions:

$$\mathcal{D}_{MK}^I \rightarrow e^{\pi i(I+K)} \mathcal{D}_{M-K}^I.$$

To see the effect of this transformation on the intrinsic wavefunctions we must decompose them into eigenfunctions of j . That is

$$\chi_{\Omega}^{\tau} = \sum_j C_{\Omega}^j \chi_{\Omega}^{\tau j},$$

and the rotation changes these eigenfunctions as follows:

$$\chi_{\Omega}^{\tau, j} \rightarrow e^{-\pi i(j+\Omega)} \chi_{\Omega}^{\tau, j}.$$

The reason for the difference in signs is the same as before.

We must now consider, separately, the two cases $K = \Omega \neq 0$ and $K = \Omega = 0$. For the first case, invariance with respect to the above rotation requires that the wavefunction be a linear combination of two products. Namely:

$$\Psi = \left(\frac{2I+1}{16\pi^2}\right)^{1/2} [\chi_K^{\tau}(\vec{\kappa}') \mathcal{D}_{M, K}^I(\theta_i) + (-1)^{I-j} \chi_{-K}^{\tau}(\vec{\kappa}') \mathcal{D}_{M, -K}^I(\theta_i)], \quad (9)$$

where the term $(-1)^j$ is to be understood to act separately on each of the j -components of the intrinsic wavefunction.

If $K = \Omega = 0$ then the product function is of the form:

$$\Psi = (2\pi)^{-1/2} \chi_0^{\tau}(\vec{\kappa}') Y_{IM}(\theta_i). \quad (10)$$

In this wavefunction, however, only certain values of I can occur. In particular, if the intrinsic wavefunction contains only even values of j , then the total I of the nucleus must also be even in order that there be a non-vanishing wavefunction. This, indeed, occurs for the low lying states in even-even nuclei.

The above symmetrization of the wavefunction which we have carried out guarantees that the parity of a nuclear state, defined by:

$$\Psi(-\vec{\kappa}) = \pi \Psi(\vec{\kappa}) = \pm \Psi(\vec{\kappa}),$$

be the same as the parity of the intrinsic wavefunction.

This can be seen quite simply; an inversion of the co-ordinates of all particles in the nucleus is equivalent to (i) an inversion of all of the co-ordinates which appear in the intrinsic wavefunction and (ii) an inversion of the nuclear surface through the origin. The first operation either leaves the wavefunction unchanged or changes its sign according to whether the parity of the intrinsic wavefunction is even or odd. The second operation is essentially equivalent to a rotation of the surface through 180° about an axis through its center, which by our construction leaves the wavefunction invariant.

With the nuclear Hamiltonian of the form (8) and the wavefunction of the form (9) or (10), the energy spectrum can be determined immediately to be:

$$E_K(I) = E_K^0 + \frac{\hbar^2}{2\mathcal{I}} [I(I+1) - 2K^2] , \quad (11)$$

where E_K^0 is a constant term independent of I which is to be chosen such that the ground state energy of the band will have the observed value. The R.P.C. term has been neglected as a small perturbation - it does not alter the form of the energy spectrum except when $K = 1/2$ (Mo57).

Figure 3-1 shows the coupling scheme for axially symmetric nuclei. We have

$$\vec{I} = K\hat{e}_3 + \vec{R} ,$$

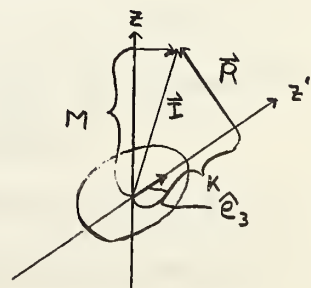


Fig. 3-1

where \hat{e}_3 is a unit vector in the direction of the symmetry axis and \vec{R} is the rotational angular momentum. From the result that $K = \Omega$, we know that the angular momentum parallel to the symmetry axis is entirely of intrinsic origin, so that \vec{R} must be perpendicular to the symmetry axis. This means that we must have $I \gg |K|$. From this result and the form of the energy spectrum we can see that the rotational band will have a ground state spin $I_0 = K$ and an energy spectrum, relative to the ground state, which is given by:

$$E_I = \frac{\hbar^2}{2\mathcal{I}} [I(I+1) - I_0(I_0+1)] . \quad (12)$$

For even-even nuclei, the lowest rotational band has $I_0 = 0$ and a spin sequence 0, 2, 4, (odd values of I are forbidden due to the inversion symmetry). It has been found experimentally that the actual energy levels of even-even nuclei in the ranges $155 \leq A \leq 185$, $A \geq 225$ and $A \approx 25$ agree very well with this prediction (Bo55, Li56, Br62).

Odd-A Nuclei also exhibit easily recognizable rotational spectra, although they are more sensitive to the details of the intrinsic motion than are even-even nuclei. According to the above equation for the energy, the spin sequence for odd-A nuclei will be $I_0, I_0 + 1, I_0 + 2, \dots$. Once again experiment has confirmed that this is indeed the correct form for the energy variation (Al56).

For the special case of $K = 1/2$ there is usually a substantial deviation from the simple rotational spectrum

as described above, since in this case the interaction term

$$R.P.C. = - \frac{\hbar^2}{2\mathcal{I}} [\vec{I} \cdot \vec{J} - I_3 J_3] ,$$

is of importance. The rotational bands with $K = 1/2$ require a special discussion because of the possibility that the intrinsic spin of the last odd nucleon may not be able to follow the rotation of the nucleus. We can see qualitatively the necessity for an additional term in the expression for the rotational energy by considering the case of a single nucleon in an $s_{1/2}$ state coupled to an even-even nucleus with $K = 0$. Since the $s_{1/2}$ state has a spherically symmetric density distribution, the energy of the system must be independent of the manner in which the angular momentum of the added nucleon is coupled to the rotational angular momentum of the even-even core. This gives rise to an energy spectrum of the form (Bo60):

$$E_K(I) = E_K^0 + \frac{\hbar^2}{2\mathcal{I}} \left[I(I+1) + (-1)^{I+1/2} (I+1/2) - 2K^2 \right]. \quad (13)$$

To determine the more general form of the energy variation for the case $K = 1/2$ we must first consider the action of the components of the total angular momentum I and the intrinsic angular momentum j upon the wavefunctions $\chi_{\alpha}^{i,j}$ and \mathcal{O}_{MK}^I . We will also need to know the commutation rules which are satisfied by these operators. We have:

$$I_x I_y - I_y I_x = i I_z , \quad (14)$$

Where the subscripts x, y, z , refer to the components in the laboratory fixed reference frame, and

$$I_1 I_2 - I_2 I_1 = -i I_3, \quad (15)$$

$$J_1 J_2 - J_2 J_1 = i J_3, \quad (16)$$

where the subscripts 1, 2, 3, denote the components in the body fixed reference frame. By making cyclic permutations of the indices the rest of the commutation relations can be obtained from those above. In addition, all components of j commute with all those of I . Equations (14) and (16) have the usual form for angular momentum commutation relations, but equation (15) has the opposite sign to that which is normally expected. The occurrence of this difference in sign can be understood in terms of the previous explanation of the difference in sign between the action of the \mathcal{D}_{MK}^I and χ_K^j functions under rotations, if we consider the fact that an arbitrary rotation of the body fixed reference frame has exactly the same effect on the \mathcal{D} functions (upon which the I 's operate) as a rotation of the laboratory fixed reference frame about the same axis and by the same angle, but in the opposite direction.

Using equations (2) and (15) one can show that (see for example Ro57)

$$(I_1 + i I_2) \mathcal{D}_{MK}^I = I_{\pm} \mathcal{D}_{MK}^I = [(I \pm K)(I \mp K + 1)]^{1/2} \mathcal{D}_{M(K \mp 1)}^I. \quad (17)$$

The intrinsic wavefunctions satisfy similar relations to the \mathcal{D} functions:

$$(j_1 \pm i j_2) \chi_K^{\tau, j} = j_{\pm} \chi_K^{\tau, j} = [(j \mp K)(j \pm K + 1)]^{1/2} \chi_K^{\tau, j}, \quad (18)$$

and
$$j_3 \chi_K^{\tau, j} = K \chi_K^{\tau, j}.$$

We now wish to use the above relations to calculate the matrix elements of the R.P.C. term. To do this we must first note that

$$\begin{aligned} \vec{I} \cdot \vec{J} &= I_1 J_1 + I_2 J_2 + I_3 J_3 \\ &= \frac{I_+ J_- + I_- J_+}{2} + I_3 J_3, \end{aligned}$$

so that
$$R.P.C. = - \frac{\hbar^2}{2J} [I_+ J_- + I_- J_+] \quad (19)$$

Using this expression for R.P.C. and relations (17) and (18) it is very easy to obtain the following relation:

$$\begin{aligned} \langle \chi_{K_2}^{\tau, j} \mathcal{O}_{M_{K_2}}^I | R.P.C. | \chi_{K_1}^{\tau, j} \mathcal{O}_{M_{K_1}}^I \rangle &= - \frac{\hbar^2}{2J} \{ [(I-K_2)(I+K_2+1)(J-K_2)(J+K_2+1)]^{1/2} \delta_{K_2, K_1-1} \\ &+ [(I+K_2)(I-K_2+1)(J+K_2)(J-K_2+1)]^{1/2} \delta_{K_2, K_1+1} \}. \quad (20) \end{aligned}$$

All other matrix elements of R.P.C. are zero.

For the special case of $K = 1/2$ equation (20) reduces to

$$\langle \chi_{1/2}^{\tau, j} \mathcal{O}_{M_{1/2}}^I | R.P.C. | \chi_{1/2}^{\tau, j} \mathcal{O}_{M_{1/2}}^I \rangle = - \frac{\hbar^2}{2J} (I+1/2)(J+1/2) \quad (21)$$

Thus, we have that the rotation particle coupling energy is of the form (Ke59):

$$E_{R.P.C.} = \frac{\hbar^2}{2J} [(-1)^{I+1/2} (I+1/2) \sum_j (-1)^{j-1/2} |C_{1/2}^j|^2 (j+1/2)] \quad (22)$$

One usually defines a parameter a such that

$$a = \sum_j (-1)^{j-1/2} |C_{1/2}^j|^2 (j+1/2), \quad (23)$$

in which case we have an energy spectrum given by:

$$E_K(I) = E_K^0 + \frac{\hbar^2}{2I} [(I+1)I - 2K^2 + \delta_{K,1/2} a (-1)^{I+1/2} (I+1/2)] . \quad (24)$$

The quantity a is referred to as the decoupling parameter since its presence in the energy relation corresponds to a partial decoupling of the particle motion from the rotational motion.

In general, the rotational spectra corresponding to the two close configurations K and $K + 1$ (with the same I) will be mixed by the R.P.C. The resulting energy spectrum is given by (Ke56):

$$E(I) = \frac{1}{2} \{ E_K(I) + E_{K+1}(I) \pm \sqrt{[E_{K+1}(I) - E_K(I)]^2 + 4A_K^2 (I-K)(I+K+1)} \} , \quad (25)$$

where $A_K = \langle K | \frac{\hbar^2}{2I} J_- | K+1 \rangle ,$

and $J_- = \sum_{particles} j$

In addition to the correction to the energy spectrum due to the R.P.C., there will be a correction arising from the coupling between the rotational and vibrational motions. This correction is usually approximated by a term of the form (Br57):

$$E_{vib,rot} = B [I(I+1) + \delta_{K,1/2} a (-1)^{I+1/2} (I+1/2)] . \quad (26)$$

With all of these corrections we have a general rotational energy spectrum which is given by:

$$E_K(I) = E_K^0 + \frac{\hbar^2}{2I} [I(I+1) + \delta_{K,1/2} a (-1)^{I+1/2} (I+1/2)] \\ + B [I(I+1) + \delta_{K,1/2} a (-1)^{I+1/2} (I+1/2)]^2 + R.P.C. \quad (27)$$

For most nuclei to which the rotational model can be applied, the first two terms of the above are sufficient to predict the observed energy spectrum.

APPLICATION TO Li^7

Li^7 and Be^7 are mirror nuclei - that is they differ only in that the odd proton in Li^7 is replaced by an odd neutron in Be^7 . If the neutron and the proton had the same masses, and if the nucleon-nucleon forces were charge independent, then this pair of mirror nuclei should have exactly the same energy level scheme. In actual fact, however, the mass difference of the neutron and proton and the coulomb repulsion between the protons are not completely negligible. The specifically nuclear forces are charge independent, i.e. they are the same whether proton - proton, proton - neutron, or neutron - neutron (Pr62). It is consequently to be expected that only the general pattern of the level system of a pair of mirror nuclei will be the same. For instance, if in one of the nuclei the first excited state has a given spin and parity, it is to be expected that a state with these properties will occur in the mirror nucleus also, at approximately, but not exactly the same excitation energy. This behaviour is indeed found in the mirror pairs such as ${}_5\text{B}_6^{11}$ - ${}_6\text{C}_5^{11}$, ${}_6\text{C}_7^{13}$ - ${}_7\text{N}_6^{13}$, and ${}_8\text{O}_9^{16}$ - ${}_9\text{F}_8^{16}$ in addition to the known levels of ${}_3\text{Li}_4^7$ - ${}_4\text{Be}_3^7$ (Aj59).

The repulsive electrostatic forces between protons

gives rise to a coulomb potential energy, E_c which reduces the binding energy due to nuclear forces. A precise calculation of this energy would require a good knowledge of the wavefunctions of the protons, but the main features of the result can be obtained with relatively simple considerations. For a spherically symmetric charge distribution $Ze \rho(r)$ the electrostatic field is

$$E(r) = \frac{ze}{r^2} \int_0^r \rho(r) r^2 dr ,$$

While the potential is

$$V(r) = ze \int_r^\infty \frac{dr}{r^2} \int_0^r \rho(r) r^2 dr ,$$

and the Coulomb energy of the whole distribution is

$$E_c = \frac{1}{2} (ze) \int_0^\infty \rho(r) V(r) 4\pi r^2 dr .$$

For a sphere of radius R of constant charge density and total charge Ze , the Coulomb energy becomes

$$E_c = \frac{3}{5} \frac{(ze)^2}{R} .$$

Using this formula the Coulomb energy correction for a mirror pair with charges Ze and $(Z-1)e$, assuming a constant nuclear radius, would be

$$\begin{aligned} \Delta E_c &= \frac{3}{5} \frac{e^2}{R} [Z^2 - (Z-1)^2] \\ &= \frac{3}{5} \frac{e^2}{R} [2Z - 1] . \end{aligned}$$

For the mirror pair ${}^7_3\text{Li} - {}^7_4\text{Be}$ this energy is 2.13 MeV. To obtain the actual energy difference between these two nuclei,

the energy equivalent to $m_p - m_n$ (= 1,294 MeV) must be added to the coulomb energy. This calculated energy difference equal to 0,84 MeV, is quite close to the measured $\text{Be}^7 - \text{Li}^7$ ground state mass difference of 0,863 MeV. This would indicate that the approximations upon which the Coulomb energy E_c was calculated are quite good as far as these two nuclei are concerned. For a detailed treatment of this energy difference various neglected effects must be considered. These include (1) non-uniformity of the average density $\rho(r)$, (2) the requirement that the charge be treated as residing on discrete protons, (3) the quantal effects of incomplete localization of protons, and (4) non-sphericity of the nucleus. These effects will not only alter the Coulomb energy correction for the ground state, but will also introduce changes in going from one excited state to another, i.e. the Coulomb energy correction will not be a constant for all levels of a nucleus.

The energy difference correction for the proposed 5,62 MeV ($3/2^-$) state of Li^7 and the corresponding state in Be^7 can be roughly estimated from the known corrections for the 7,47 MeV ($5/2^-$), 6,58 MeV ($5/2^-$), 4,63 MeV ($7/2^-$), and 0,478 MeV ($1/2^-$) levels. The correction as estimated in this manner is 0,73 MeV, i.e. the coulomb energy correction is 130 keV less for this state than for the ground state. This means that the level in Be^7 which corresponds to the predicted

5.62 MeV ($3/2^-$) level of Li^7 should have an excitation energy of about 5.5 MeV.

It is thus expected that an analysis of Li^7 should hold, insofar as its general features are concerned, for Be^7 also. Li^7 has been dealt with by Chesterfield and Spicer since more data are available on it than on Be^7 .

Chesterfield and Spicer (Ch63) have calculated a theoretical energy spectrum for Li^7 based on the rotational model which was described above. In order to carry out the calculations it was necessary for them to assume a specific form for the intrinsic Hamiltonian $H_{\text{intrinsic}}(\vec{\pi}')$ in equation (3); to this end the "Nilsson Potential" was assumed. This potential is obtained by starting with an anisotropic oscillator potential and adding two terms; $D\vec{\ell}\cdot\vec{\ell}$ which favours high ℓ values, and $C\vec{\ell}\cdot\vec{J}$ a simple form for the spin orbit coupling. The resulting Hamiltonian then has the form:

$$H_{\text{intrinsic}}(\vec{\pi}') = \frac{p^2}{2m} + \frac{m}{2} (\omega_x^2 x^2 + \omega_y^2 y^2 + \omega_z^2 z^2) + C\vec{\ell}\cdot\vec{J} + D\vec{\ell}\cdot\vec{\ell}. \quad (28)$$

For the special case of axial symmetry the ω 's are related as follows:

$$\begin{aligned} \omega_x^2 &= \omega_y^2 = \omega_o^2 (1 + \frac{2}{3} \delta), \\ \omega_z^2 &= \omega_o^2 (1 - \frac{4}{3} \delta), \end{aligned}$$

where δ is a measure of the distortion of the nucleus.

Since nuclear matter is usually considered to be incompressible we must have the deformations of the nucleus taking place at

constant volume, - this leads to the requirement that

$$\omega_0(\delta) = \tilde{\omega}_0 (1 + 4/3 \delta - 1/27 \delta^3)^{-1/6}. \quad (29)$$

$\tilde{\omega}_0$ is the value of $\omega_0(\delta)$ for no deformation ($\delta = 0$).

Nilsson (Ni55) has given an estimate of $\tilde{\omega}_0$,

$$\hbar \tilde{\omega}_0 = 41 A^{-1/3},$$

however, Chesterfield and Spicer rather than using this value chose $\hbar \tilde{\omega}_0$ such that the best overall fit to the known level scheme was obtained. The value which they used (22.4 MeV) is close to that obtained from $41 A^{-1/3}$ (21.5 MeV).

It is customary to define two new parameters which simplify calculation

$$\begin{aligned} \chi &= -C / 2\hbar \tilde{\omega}_0, \\ \eta &= \frac{\delta \omega_0(\delta)}{\chi \tilde{\omega}_0}, \end{aligned}$$

where C is the coefficient of the $\vec{l} \cdot \vec{s}$ term in the nuclear potential.

For each value of the distortion η a wave function and a level order is obtained (see for example the plots of Nilsson). In order to reproduce, as closely as possible, the energy levels and wavefunctions as predicted by the shell model it is necessary to choose the coefficient D in formula (28) to be equal to zero for particles filling the s, p, and d shells.

Using the above considerations Nilsson has shown that for a particular orbit characterized by quantum numbers N, Ω

the nuclear Hamiltonian $H_{\text{nth}}(\pi')$ has eigenvalues

$$E_K^0 = (N_K + 3/2) \hbar \omega_0(\delta) + \kappa \hbar \omega_0 r_K^{N_K}(\delta) . \quad (30)$$

Here N is the total number of oscillator quanta, Ω is the projection of the total intrinsic angular momentum j on the nuclear symmetry axis as defined in the previous section, K numbers the different eigenvalues of each Nilsson orbital, and $r_K^{N_K}$ is an eigenvalue defined and tabulated by Nilsson. This eigenvalue arises when the non-spherically symmetric portion of the Hamiltonian in equation $(H_{\text{nth}} = \frac{p'^2}{2m} - \frac{m}{2} \omega_0^2 r^2)$ is diagonalized for a sequence of η values.

Chesterfield and Spicer calculated the energy spectrum as given by equations (27) and (30) for various values of κ and found that the most satisfactory overall agreement with the known data was obtained for $\kappa = 0.08$, the value suggested by Mottleson and Nilsson (Mo59). $\frac{\hbar}{2\pi}$ was adjusted so as to give a best fit to the available data. (It was noted that these values of $\frac{\hbar^2}{2\pi}$ varied with the deformation in approximately the manner predicted by Skyrme (Sk57)). Finally, it was determined that both the R.P.C. and the rotation - vibration interaction terms were negligible perturbations to the rotational energy spectrum.

In calculating the energy level scheme, states obtained from many particle excitations were neglected on the grounds that they would be more difficult to form than would single particle excitations.

The energy spectrum obtained from equation (27) is correct only if no pairs are made or broken in the course of the excitation of the nucleus, but the intrinsic state corresponding to the fourth excited rotational band (the second band based on $K = 1/2^+$) arises when a pair of protons in the s shell is broken and a pair is made in the p shell.

This pairing energy difference between the s and p shells can plausibly be obtained from the difference in energy between the $\text{He}^4 (\gamma, p)$ and $\text{Be}^8 (\gamma, p)$ thresholds. The energy required to remove a proton from the s shell is given by the $\text{He}^4 (\gamma, p)$ threshold, while that required to remove a proton from the p shell is presumably given by the $\text{Be}^8 (\gamma, p)$ threshold since Be^8 , which can be described as two virtually free alpha-particles (bound by - 94 keV), one composed of s nucleons and the other of p nucleons, has a threshold that is lower than the $\text{He}^4 (\gamma, p)$ threshold. However, Be^8 is unstable, breaking up into two alpha-particles in less than 4×10^{-15} seconds. This means that a direct measurement of the $\text{Be}^8 (\gamma, p)$ threshold is not possible. Chesterfield and Spicer have estimated this threshold using the mass values given by Konig et al (Ko62), i.e. they assumed that the $\text{Be}^8 (\gamma, p)$ threshold was given by:

$$\begin{aligned} \text{Be}^8 (\gamma, p) \text{ threshold} = & \text{Mass} (\text{Be}^7) + \text{Mass} (\text{proton}) \\ & - \text{Mass} (\text{Be}^8), \end{aligned}$$

The pairing energy difference, as estimated in this manner,

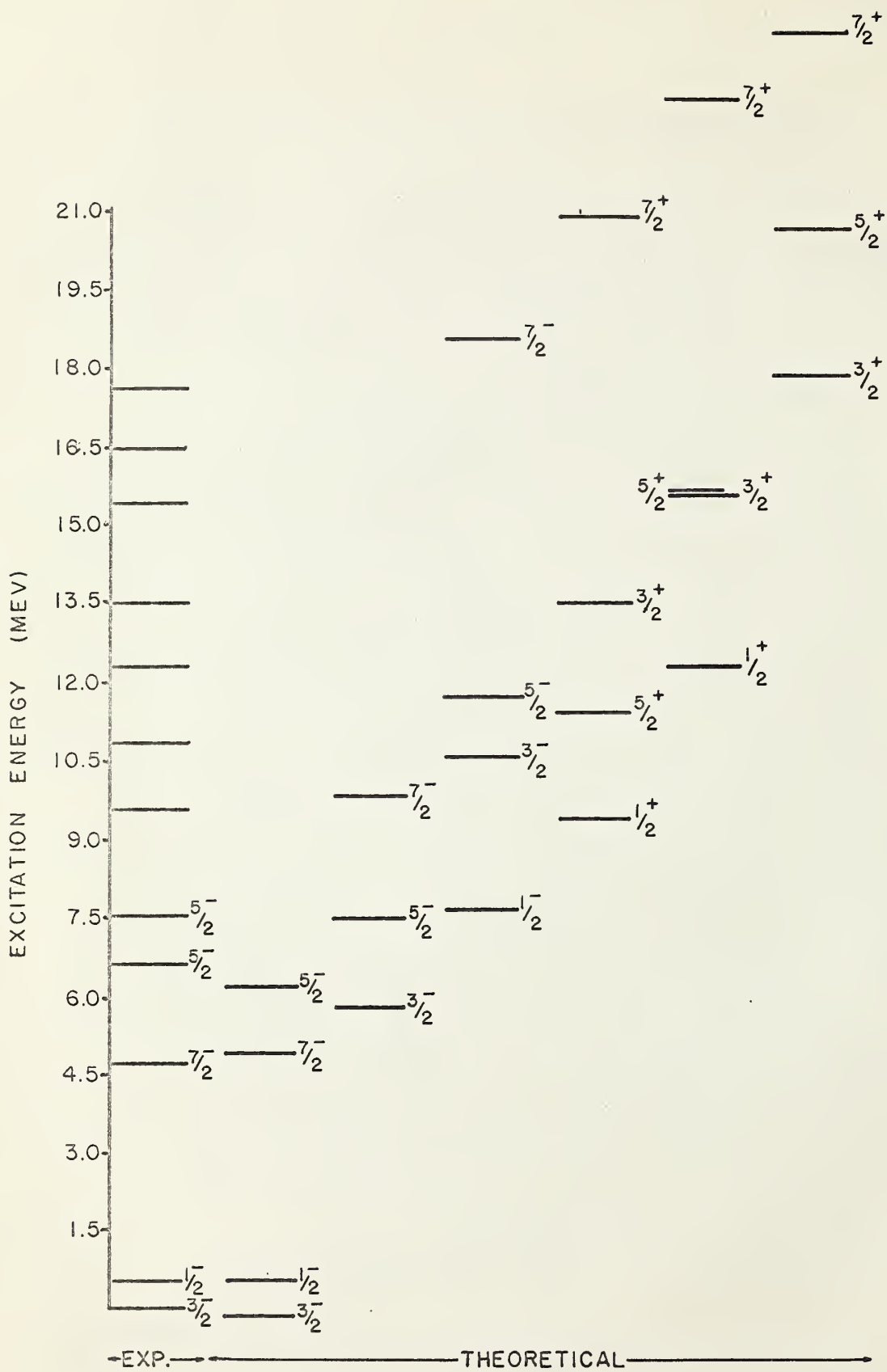


Figure 3-2

is 2.56 MeV for the s and p shells of Li^7 .

In figure 3-2 is shown the predicted level scheme along with the Li^7 levels known from experiment.

It will be noted that the first three states are all predicted to be members of a rotational band based on the 0.478 MeV ($1/2^-$) state, and have spins $3/2^-$, $1/2^-$, and $7/2^-$. The $I^\pi = 5/2^-$ member of this band is predicted to be at an excitation energy of 6.27 MeV. Chesterfield and Spicer identify this level with the broad 6.58 MeV ($3/2^+$) level. To substantiate this they give recently published experimental evidence (To62) to show that the spin of this state could very well be $5/2^-$.

With this interpretation of the 6.5 MeV state it is then necessary to postulate that the 7.47 MeV ($5/2^-$) state is a member of a rotational band whose base state is at an excitation energy of 5.62 MeV, and has $I^\pi = 3/2^-$. It is the question of the existence of this level which it was hoped the present experiment would be able to resolve.

The levels in the two rotational bands with base state spins equal to $1/2$ and positive parity (the third and fourth excited rotational bands) are in very good agreement with experiment as is exhibited by table 3-1.

There is no way at present to check the predictions of the second excited rotational band, which is based on an $K = 1/2^-$ state since no odd parity levels have been found in

the region with excitation energies between 8 MeV and 15 MeV. The experimental levels, which lie in this region, are tabulated in table 3-1. These levels were found by means of the reaction $\text{Li}^7 (\gamma, n)$ and are presumed to be positive parity states since the bremsstrahlung which was used to induce this reaction should excite, primarily, positive parity levels with spins equal to $1/2$, $3/2$, or $5/2$.

TABLE 3-1

Levels of Li^7 (in MeV) from $\text{Li}^7(\gamma, n)\text{Li}^6$

Predicted levels		Bo53	Reference Ry58	Ch63
9,43	(1/2+)	9,6	9,66 \pm 0,04	
11,40	(5/2+)	10,8		
12,27	(1/2+)	12,4		12,25
13,53	(3/2+)	14,0		13,5
15,57	(3/2+)			15,4
15,57	(5/2+)			16,5
17,95	(3/2+)	17,5		17,75

It is to be expected that a number of the theoretically predicted levels should be in agreement with the experimental levels, since the parameters $\hbar\omega_0$ and \mathcal{K} have been adjusted for the best overall fit to the experimental data. In addition, the moment of inertia for each band has also been adjusted to give the best fit to the experimental levels within the

band. Thus, a relatively good fit between theory and experiment is expected for at least the three low lying levels in the ground state rotational band. What is so surprising about this application of the rotational model to Li^7 is the very good agreement between experiment and theory for the positive parity levels with a relatively high excitation energy (9 MeV - 18 MeV). This latter agreement would lead one to suspect that there is good justification for thinking that the rotational model can be applied to Li^7 .

In addition to a level scheme for Li^7 , the rotational model has also predicted, correctly, the ground state electromagnetic moments, the mean lifetime for the de-excitation of the first excited state by gamma ray emission, the ratio of the E2/M1 mixing for this decay, and the log (ft) values for the β -decay of Be^7 to Li^7 .

SECTION 4. THE EXISTENCE OF THE PROPOSED NEW LEVEL OF Be^7

In a search for the Be^7 mirror analogue to the 5.62 MeV ($3/2^-$) level of Li^7 , the yield of gamma rays from the reaction $\text{Li}^6(p,\gamma)\text{Be}^7$ was investigated, but it showed no evidence of a resonance in the range of proton bombarding energies $E_p = 200$ keV to $E_p = 450$ keV. This would indicate that, if the state is to be found in this region, it either has an extremely low cross section for de-excitation by gamma rays, or else the state is very broad and would consequently not be expected to show a sharp resonance.

The spectra taken at $E_p = 800$ keV and $E_p = 400$ keV are essentially in agreement with the results of Warren et al for the decay of the broad 6.35 MeV level of Be^7 , although it would appear that there was more fluorine contamination on the targets used in this experiment than on those of Warren et al. However, a spectrum taken at $E_p = 300$ keV shows a different character than those taken at higher energies, indicating that some other process is being observed. This may be the decay of the proposed $3/2^-$ level, or else it could be the presence of some unknown contaminants. From penetrability considerations the yield of gamma rays from the reaction $\text{Li}^6(p,\gamma)\text{Be}^7$ decreases rapidly as the

proton bombarding energy is lowered, but the penetrability factor for protons on contaminants with a Z higher than that of lithium ($Z = 3$) will decrease more rapidly. This will tend to make the presence of probable contaminants less important at lower energies.

The spectra taken at $E_p = 800$ keV and $E_p = 400$ keV are explainable in terms of the gamma rays from the 6.35 MeV level of Be^7 and the 6.13 MeV level of O^{16} . In the spectrum taken at $E_p = 300$ keV (Figure 2-7b), however, there would appear to be gamma rays present with energies between 4.4 MeV and 5.4 MeV, in addition to those expected from the decay of the 6.35 MeV level of Be^7 .

It may be possible to explain the spectrum of Figure 2-7b in terms of the decay of proposed $3/2^-$ state to the ground, first, and second excited states of Be^7 . If such is the case, then the $3/2^-$ level predicted by Chesterfield and Spicer is a broad level which merges with the 6.35 MeV level at approximately 5.9 MeV. This provides a plausible explanation of the observed facts regarding the yield curve of Figures 2-7a, 2-7b, and the spectra taken at the bombarding energies $E_p = 800$ keV and $E_p = 400$ keV.

The spectrum of Figure 2-7b was taken for an incident charge of 3×10^{-3} coulombs (approximately 5 times the integrated beam current which produced the spectra of Figures 2-5 and 2-6). Thus the effect observed in Figure 2-7b is

very weak, and contains insufficient data to make a confident decision as to the existence of the proposed new state.

BIBLIOGRAPHY

- Aj59 F. Ajzenberg-Selove, T. Lauritsen, Nuc. Phys. 11
(1959) 1.
- Al56 K. Alder, A. Bohr, T. Huus, B.R. Mottelson, A.
Winther, Rev. Mod. Phys. 28 (1956) 432.
- Ba55 S. Bashkin, R.R. Carlson, Phys. Rev. 97 (1955) 1245.
- Bo53 A. Bohr, B.R. Mottelson, Mat. Fys. Medd Dan. Vid.
Selsk. 27 No. 16 (1953).
- Bo55 A. Bohr, B.R. Mottelson. "Collective Nuclear Motion
and the Unified Model". Chapt. xvii P. 483 of
Beta and Gamma Ray Spectroscopy. Edited by K.
Seigbahn. North Holland Publishing Co. (1955).
- Bo60 A. Bohr, B.R. Mottelson. "Collective Motion and
Nuclear Spectra:.. Chapt. vi-c P. 1009 of Nuclear
Spectroscopy Part B. Edited by Fay Ajzenberg-
Selove. Academic Press. (1960).
- Br57 C.P. Browne. Bull Amer. Phys. Soc. 2 (1957) 350.
- Br57a D.A. Bromley, H.E. Gove, A.E. Litherland, Can. J.
Phys. 35 (1957) 1057.
- Br62 D.W. Braben, L.L. Green, J.C. Willmott, Nuc. Phys.
32 (1962) 584.
- Ch63 C.M. Chesterfield, B.M. Spicer, Nuc. Phys. 41 (1963)
675.
- Cu39 S.C. Curran, J.E. Strothers. Proc. Roy. Soc. (London)
A172 (1939) 72.
- Er54 P. Erdos, P. Stoll, M. Wachter. Nuovo Cimento Series
9 Vol 12 P. 639 (1954).
- Er54a Erdman, Warren, James, Alexander. Phys. Rev. 96 (1954)
858(A).

- Ge56 R.W. Gelenas, S.S. Hanna, Phys. Rev, 104 (1956) 1681
- Go59 H.E. Gove, "Resonance Reactions, Experimental", Chapt. vi of Nuclear Reactions Vol. 1, Edited by P.M. Endt and M. Demeur, North Holland Publishing Co, (1959),
- Ke56 A.K. Kerman, Mat. Fys. Medd Dan. Vid. Selsk 29 No, 15 (1956),
- Ke59 A.K. Kerman, "Nuclear Rotational Motion", Chapt. x P. 427 of Nuclear Reactions Vol. 1, Edited by P.M. Endt and M. Demeur, North Holland Publishing Co, (1959),
- Ko62 L.A. König, J.H.E. Mattauch, A.H. Wapstra, Nuc Phys, 31 (1962) 1
- Le57 C.A. Levinsen, M.K. Banerjee, Ann. of Phys 2 (1957) 471,
- Li56 A.E. Litherland, E.B. Paul, Bartholomew, H.E. Green, Phys. Rev. 102 (1956) 308.
- Ma56 J.B. Marion, G. Weber, F.S. Mozer. Phys. Rev. 104 (1956) 1402.
- Ma57 D.R. Maxson, E.F. Bennett, Bull, Amer. Phys. Soc. 2 (1957) 180.
- Mo57 S.A. Moskowski, "Models of Nuclear Structure", Vol. 34 P. 411 of Handbuch Der Physik. Edited by S. Flugge, Springer-Verlag Publishing Co. (1957),
- Mo59 B.R. Mottelson, S.G. Nilsson, Mat. Fys. Skr. Dan Vid. Selsk 1, No. 8 (1959),
- Ni55 S.G. Nilsson, Mat. Fys. Medd, Dan Vid. Selsk 29, No. 16 (1955),
- Pr62 M.A. Preston, Chapt 2 and Chapt 5 of Phys. of the Nucleus Addison-Wesley Publishing Co. (1962),
- Ra50 J. Rainwater, Phys. Rev. 79 (1950) 432.
- Ra57 G. Rakavy, Nuc. Phys. 4 (1957) 375.
- Re63 A. Reedyk, Private Communication.

- Ro57 M.E. Rose, Elementary Theory of Angular Momentum,
John Wiley & Sons (1957) P. 22ff.
- Ry58 T.W. Rybka, L. Katz, Phys. Rev. 110 (1958) 1123.
- Sk57 A.K. Skyrme, Proc. Phys. Soc. A70 (1957) 433.
- St54 P. Stoll, Helv. Phys. Acta 27 (1954) 395.
- To62 T.A. Tombrello, P.D. Parker, C.A. Barnes, Bull.
Amer. Phys. Soc. 7 (1962) 268.
- Wa56 J.B. Warren, T.K. Alexander, G.B. Chadwick, Phys.
Rev. 101 (1956) 242.

B29811